Supporting Information

" Intramolecular Michael Additions in Uridine Derivatives. Isolation of the labile 5'O-C6 Cyclonucleoside."

Arnaud Gissot,*[a] Stéphane Massip,[b] and Philippe Barthélémy *[a]

[a] *Univ. Bordeaux, CNRS, INSERM, ARNA, UMR 5320, U1212, F-33000 Bordeaux, France.*

e-mail: arnaud.gissot@u-bordeaux.fr ; philippe.barthelemy@inserm.fr. Tel: +33 557 574 634

[b] *Univ. Bordeaux, CNRS UMS 3033, INSERM US001, IECB, 2 Rue Escarpit, F-33600 Pessac, France*

NMR and mass spectra of the cyclonucleosides **1**, **2a-b**, **3a-b** and the disulfide **7**.

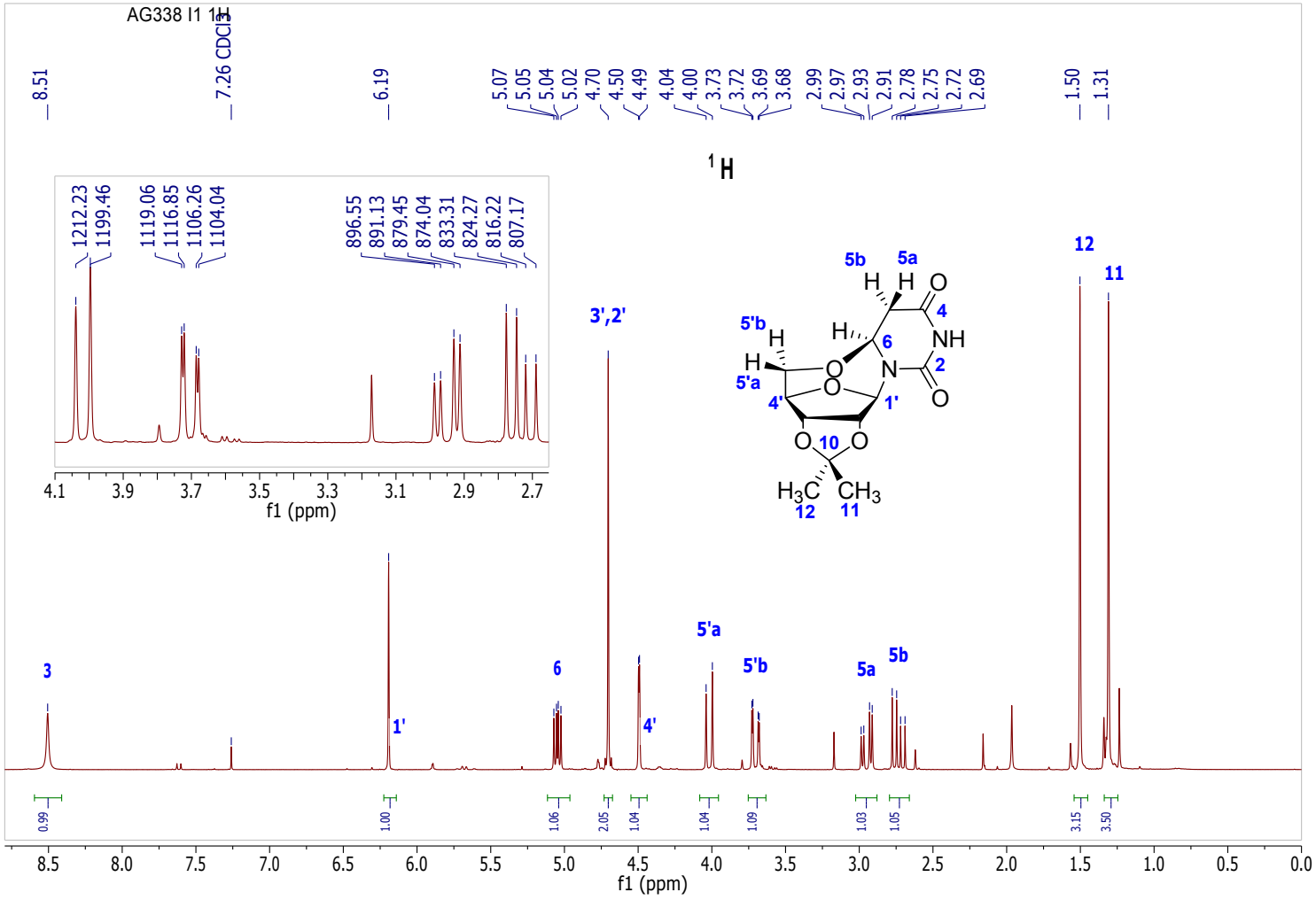

Figure S1. ^{1}H spectrum of O-cyclonucleoside (**1**)

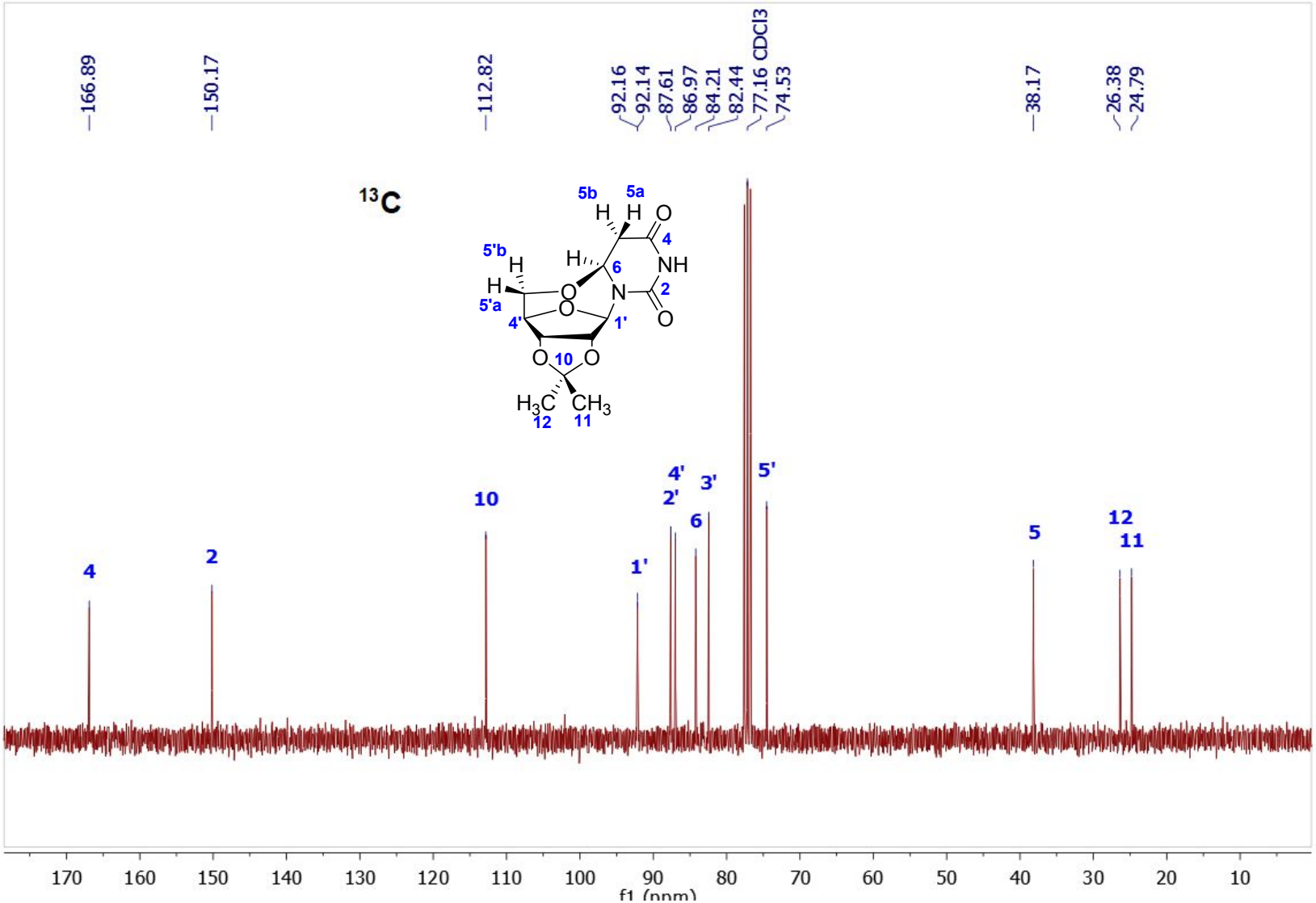

Figure S2. ^{13}C spectrum of O-cyclonucleoside (**1**)

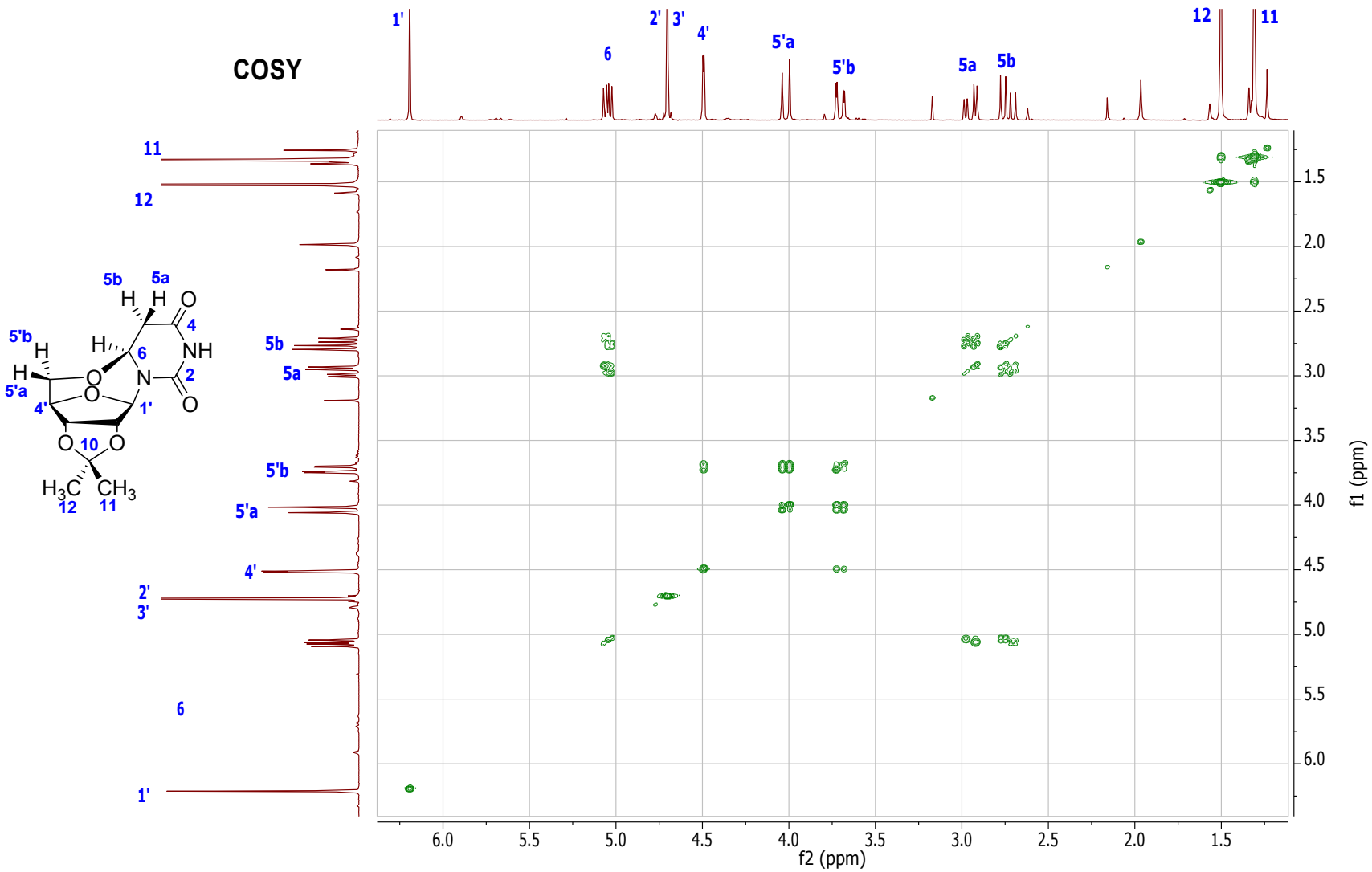

Figure S3. COSY spectrum of O-cyclonucleoside (**1**)

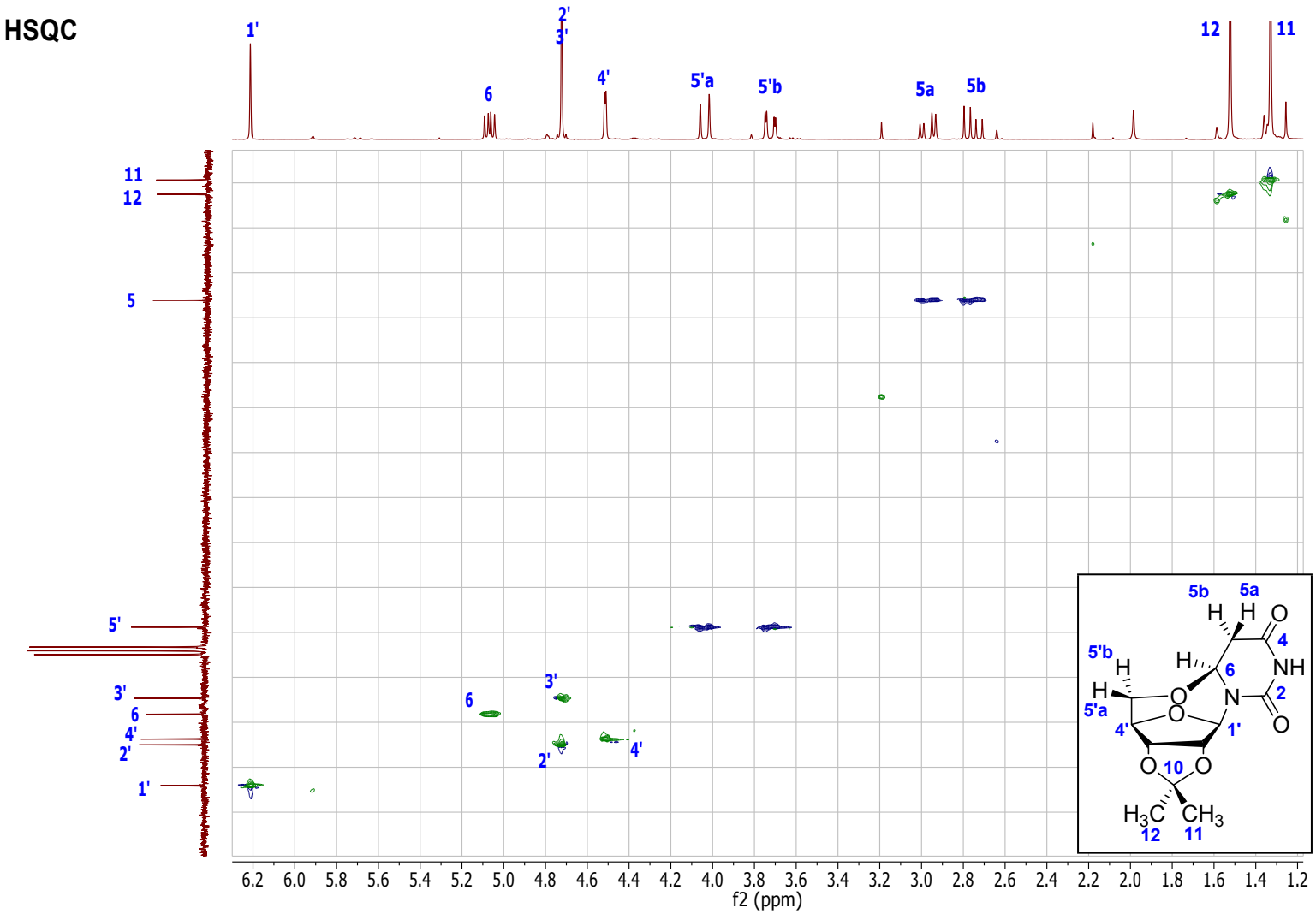

Figure S4. HSQC spectrum of O-cyclonucleoside (**1**)

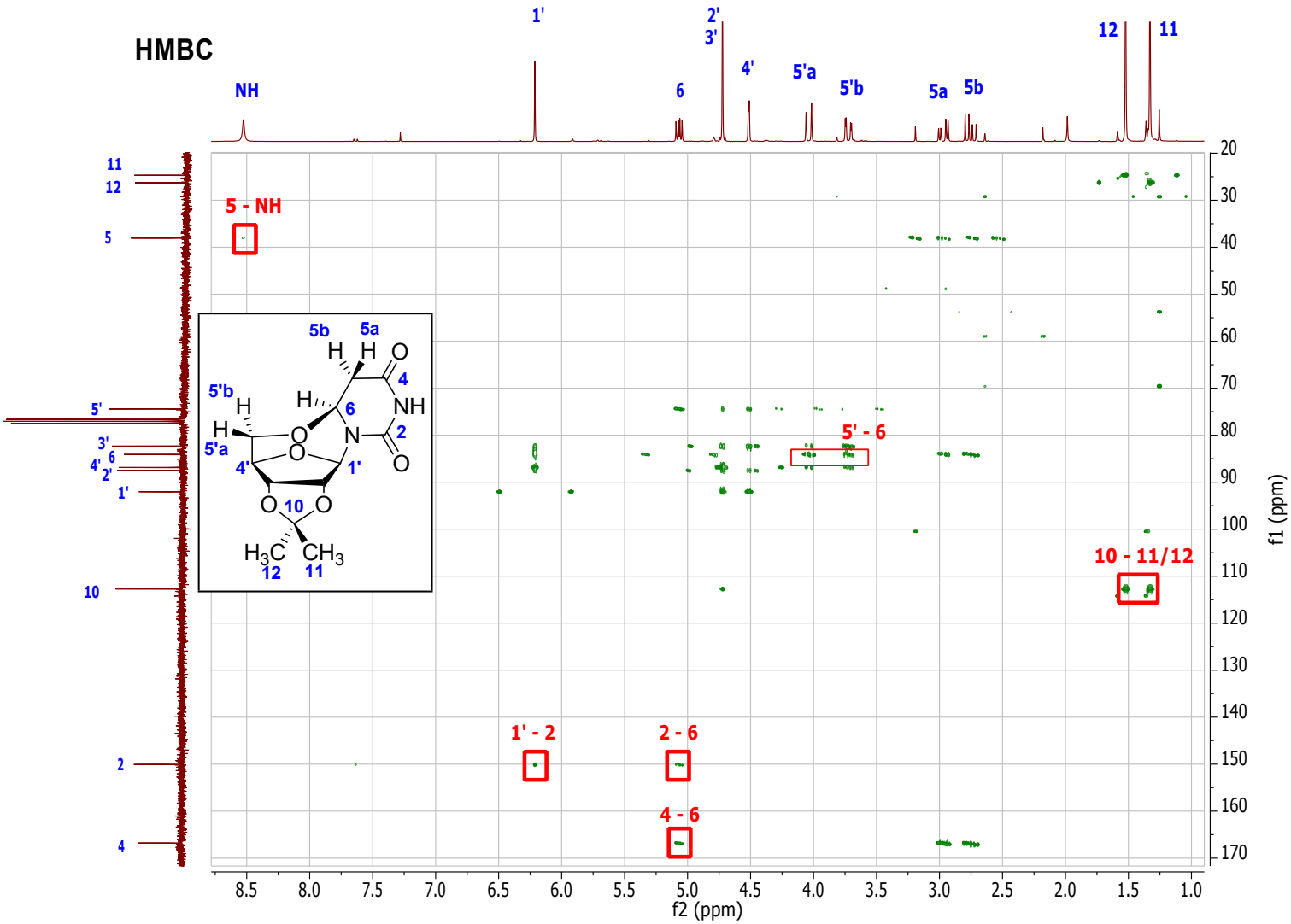

Figure S5. HMBC spectrum of O-cyclonucleoside (**1**)

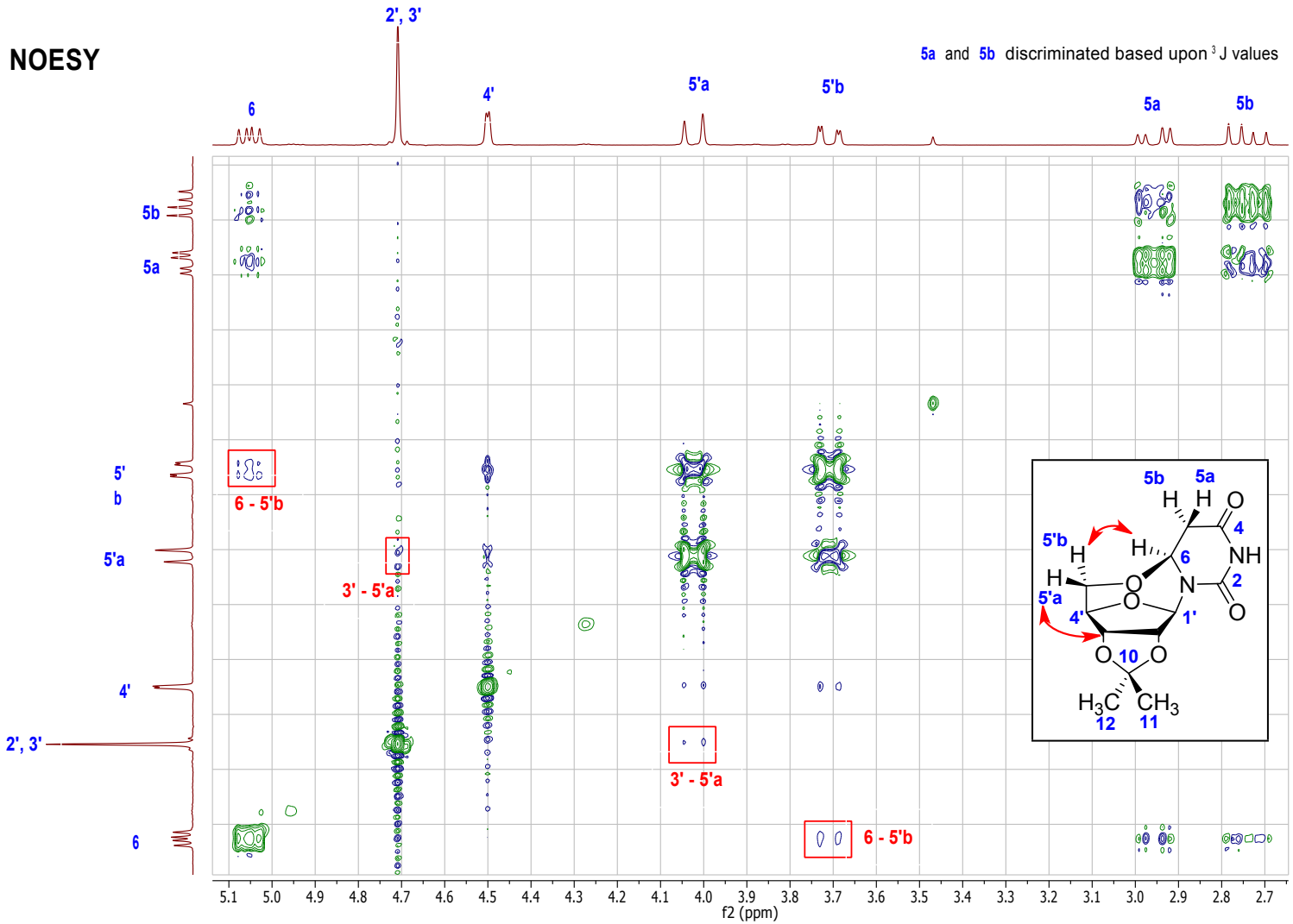

Figure S6. ROESY spectrum of O-cyclonucleoside (**1**)

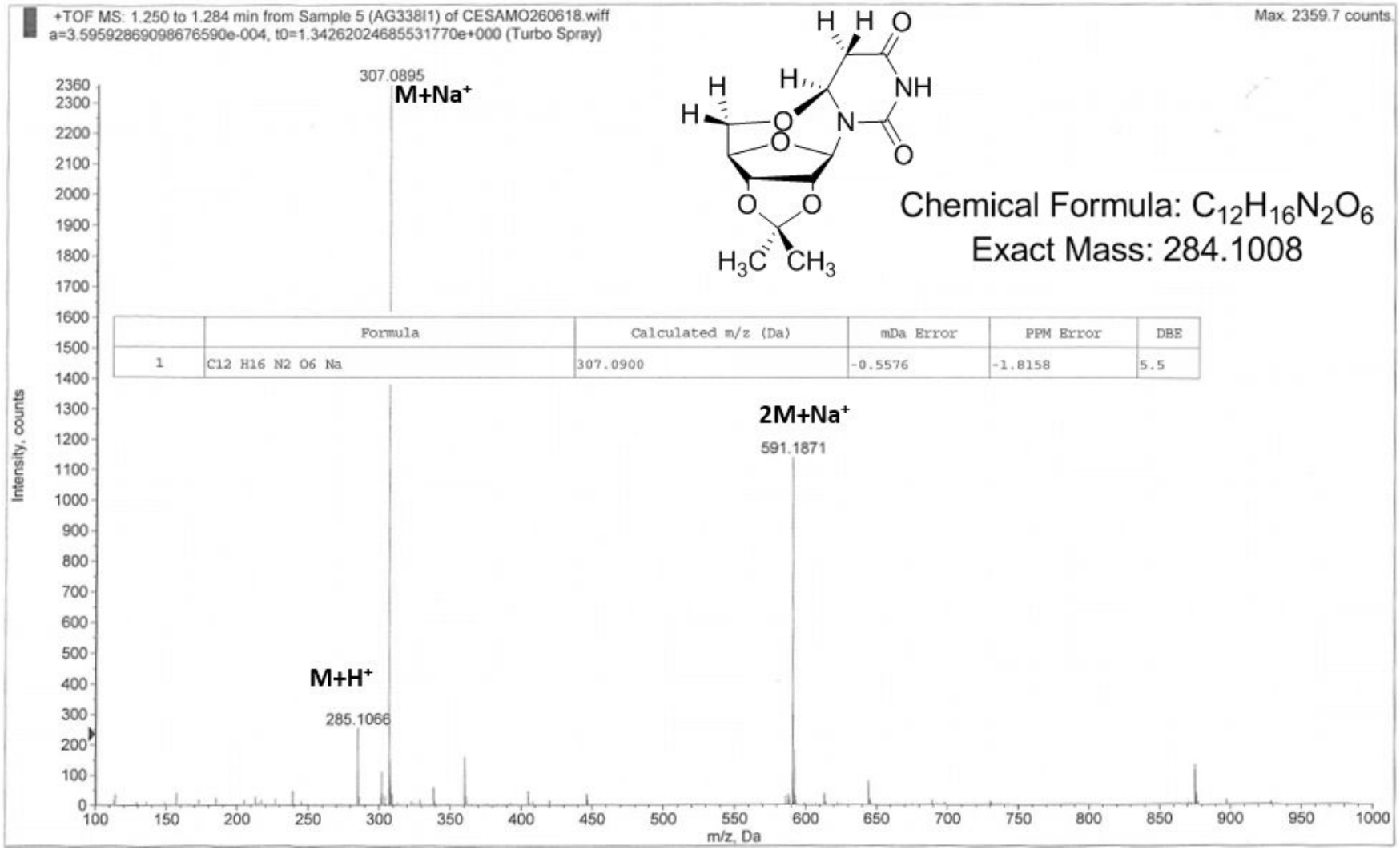

Figure S7. HRMS of O-cyclonucleoside (**1**)

N-cyclonucleoside (**2a**)

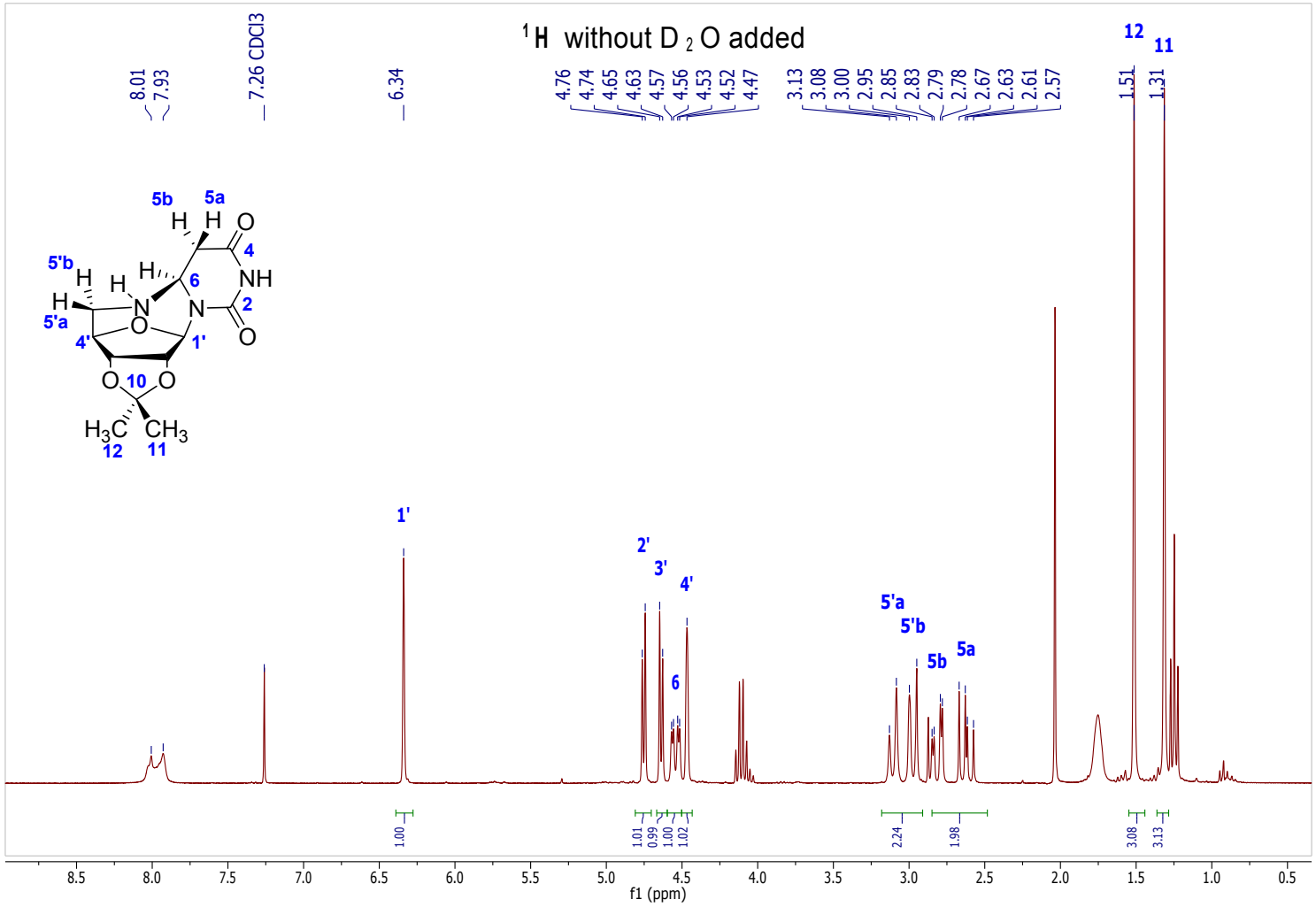

Figure S8. ^{1}H spectrum of N-cyclonucleoside (**2a**)

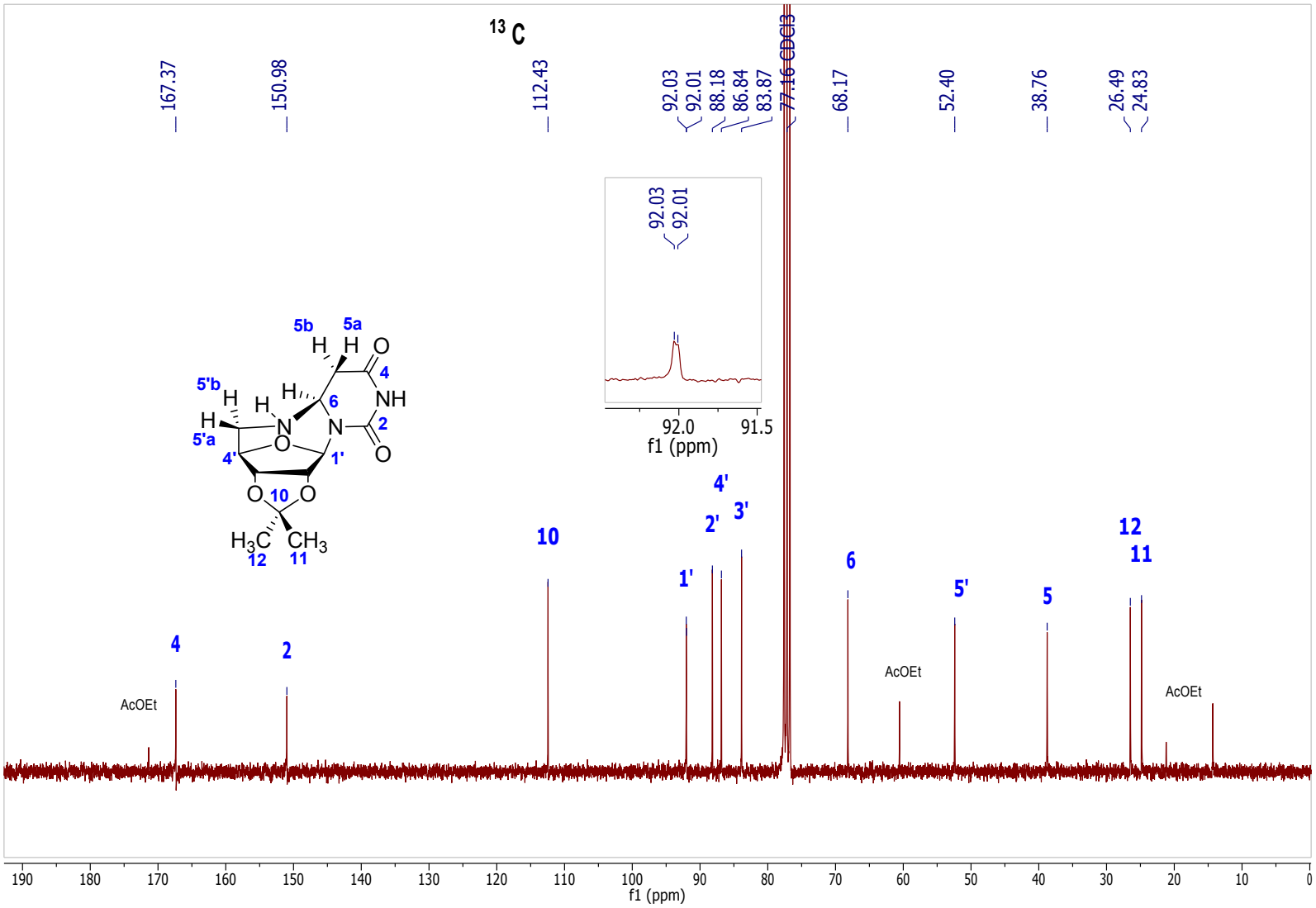

Figure S9. ^{13}C spectrum of N-cyclonucleoside (**2a**)

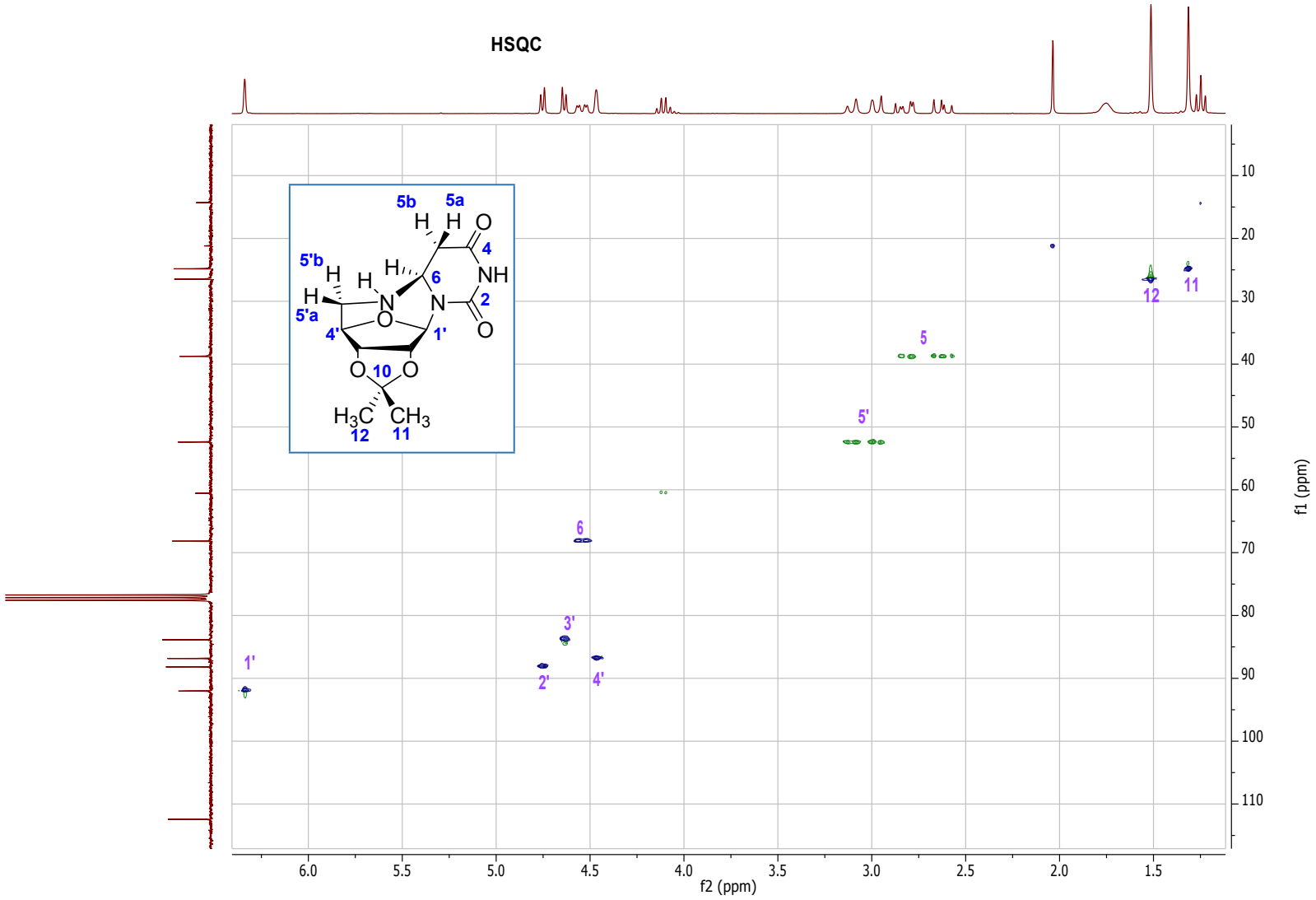

Figure S10. HSQC spectrum of N-cyclonucleoside (**2a**)

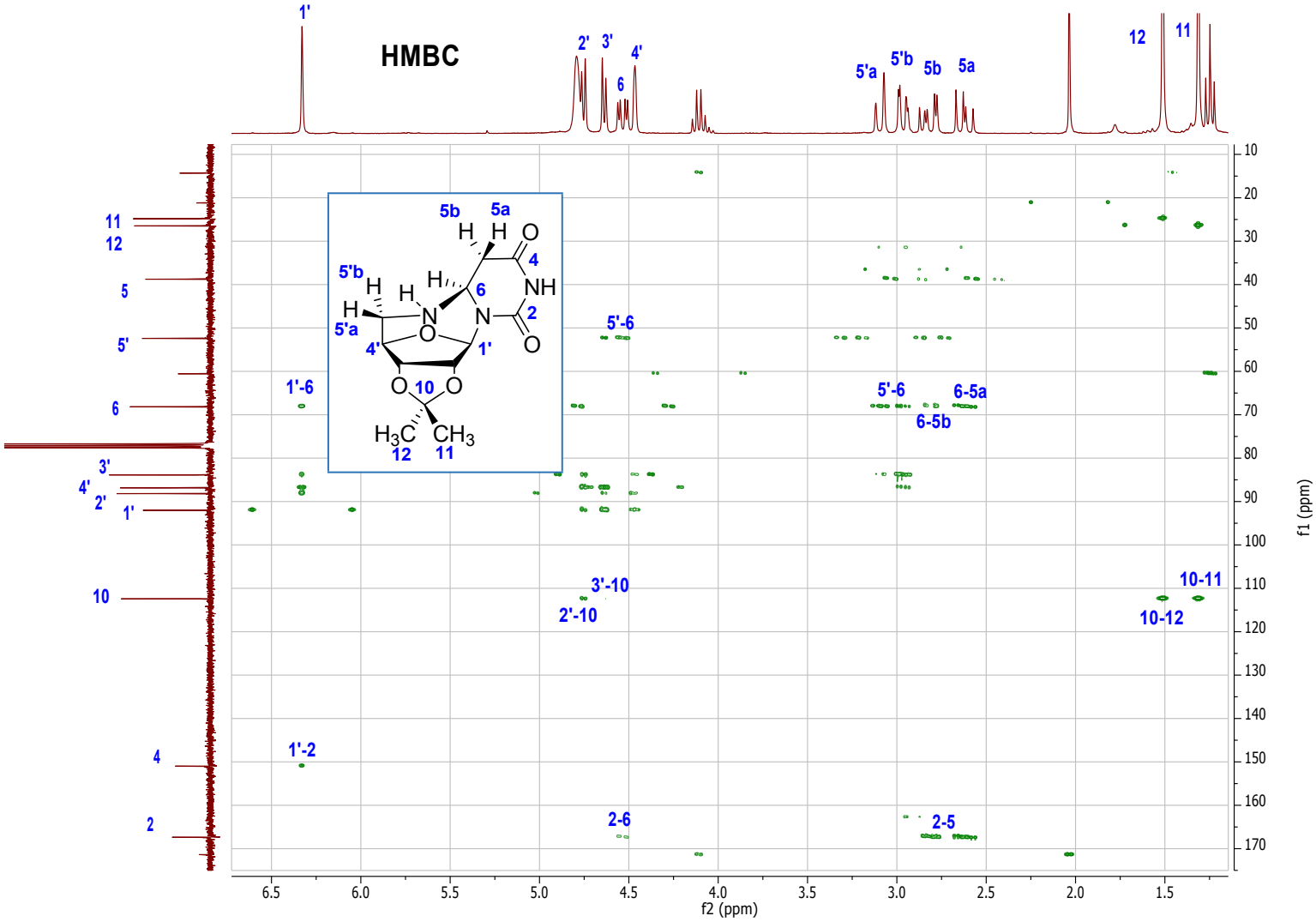

Figure S11. HMBC spectrum of N-cyclonucleoside (**2a**)

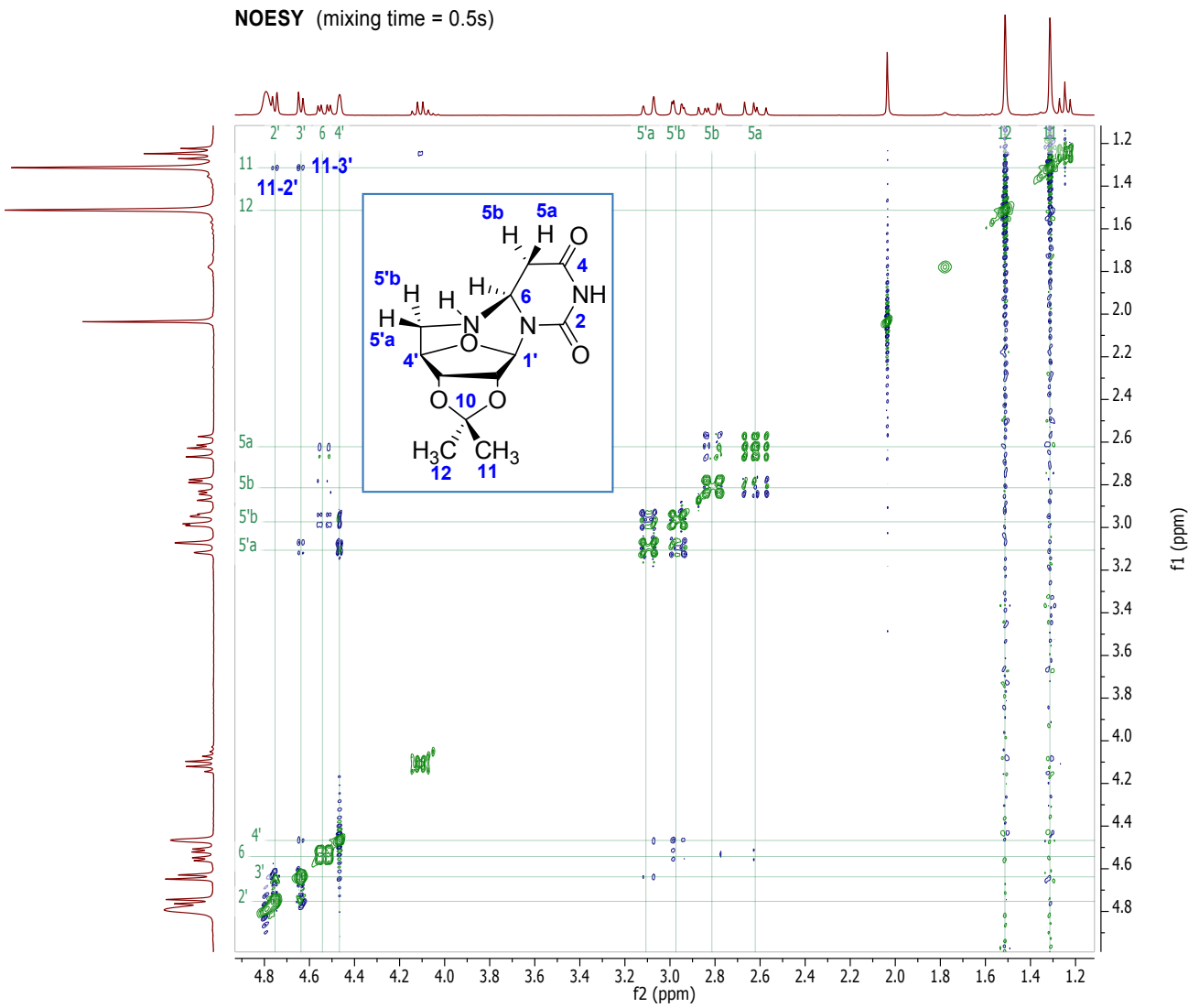

Figure S12. ROESY spectrum of N-cyclonucleoside (**2a**)

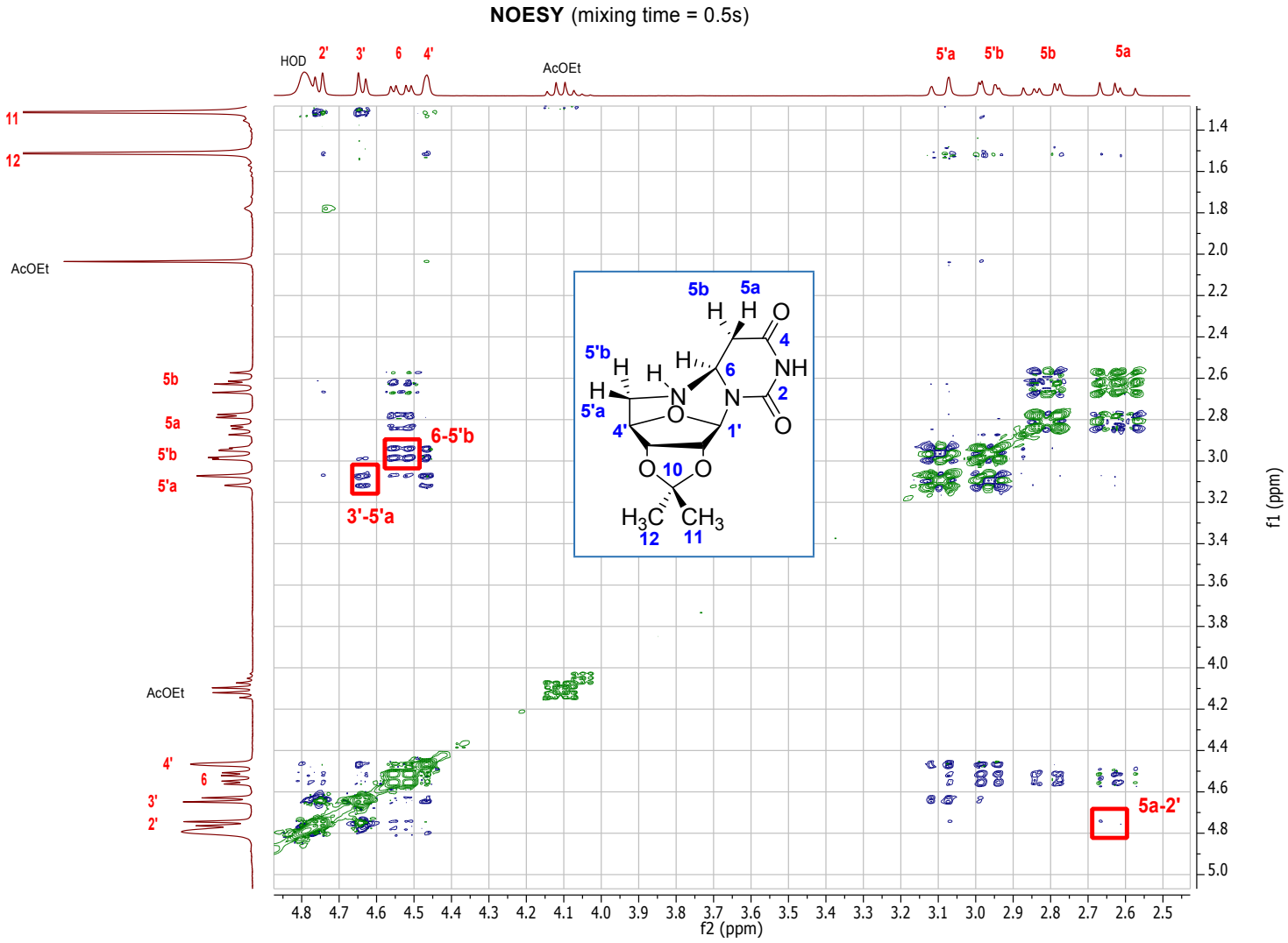

Figure S13. ROESY (blow-up) spectrum of N-cyclonucleoside (**2a**)

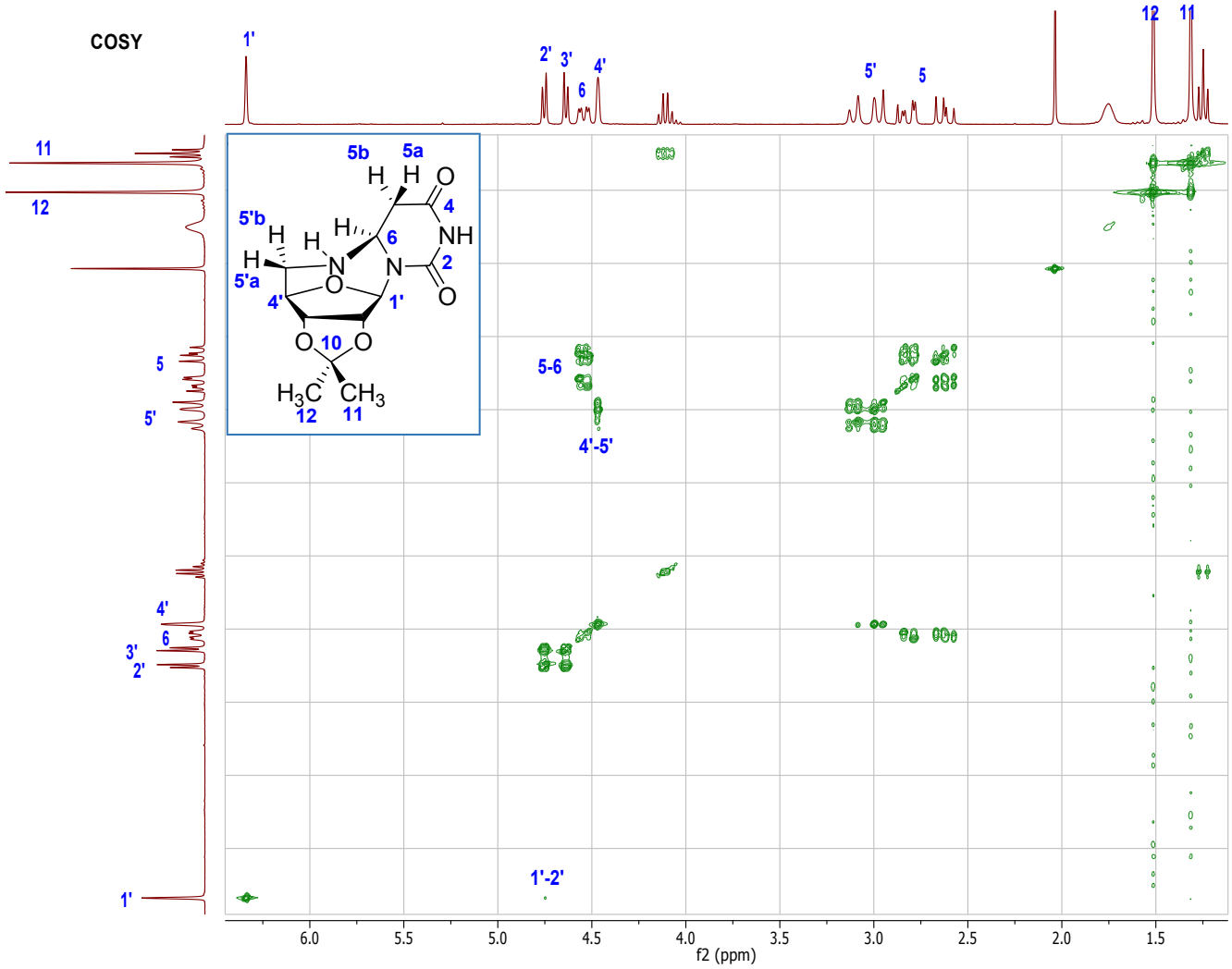

Figure S14. COSY spectrum of N-cyclonucleoside (**2a**)

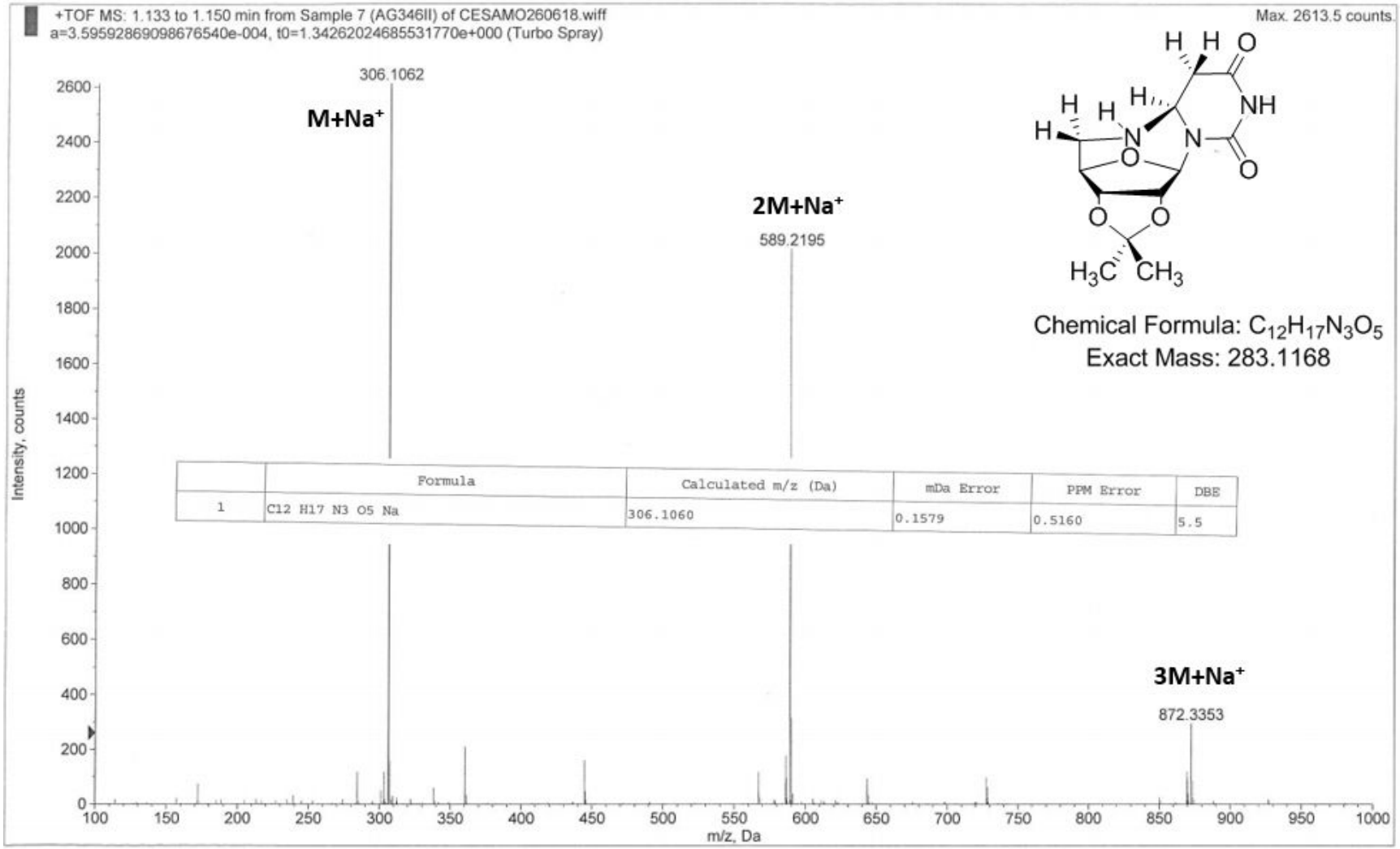

Figure S15. HRMS of N-cyclonucleoside (**2a**)

N-cyclonucleoside (**2b**)

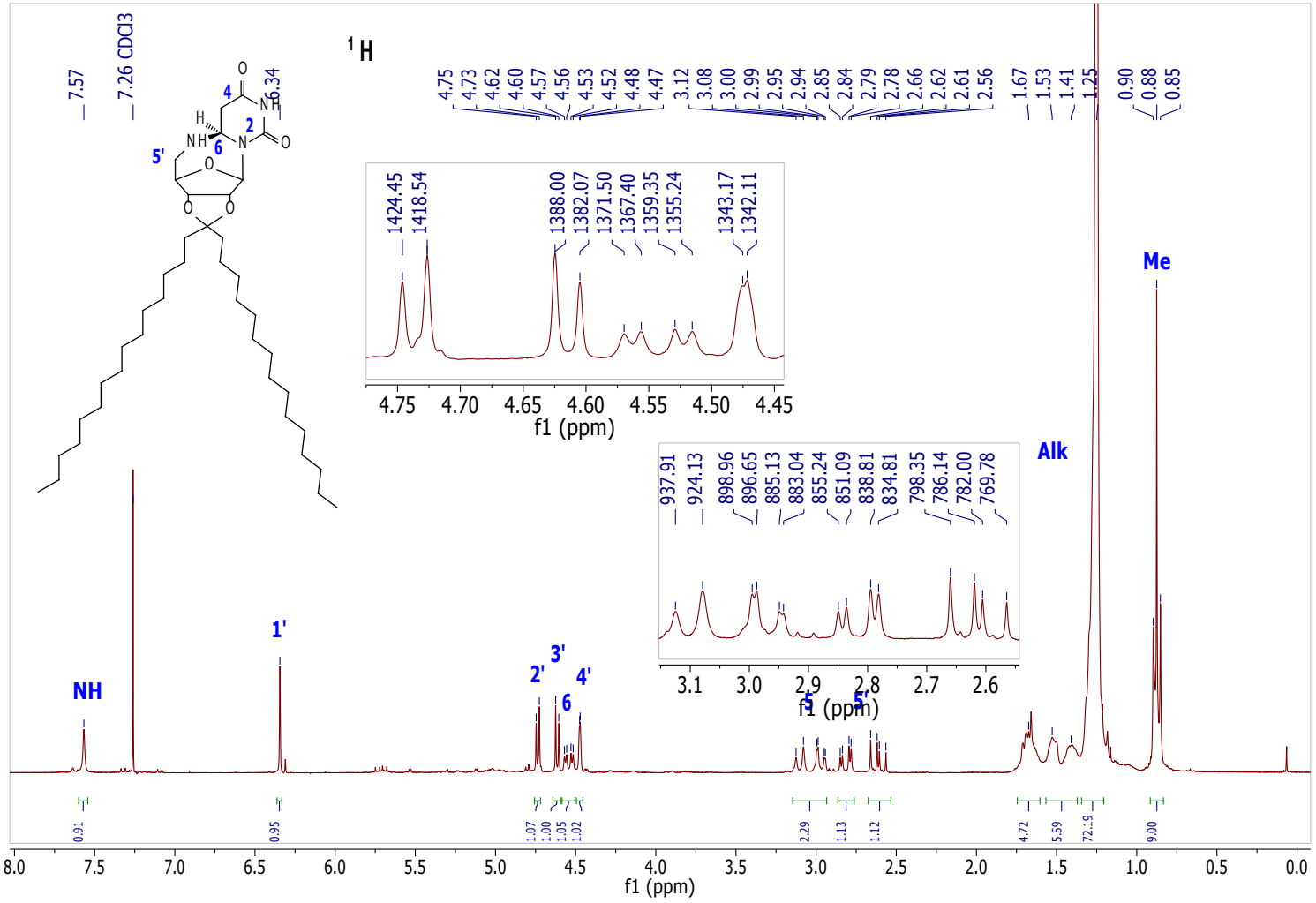

Figure S16. ^{1}H spectrum of N-cyclonucleoside (**2b**)

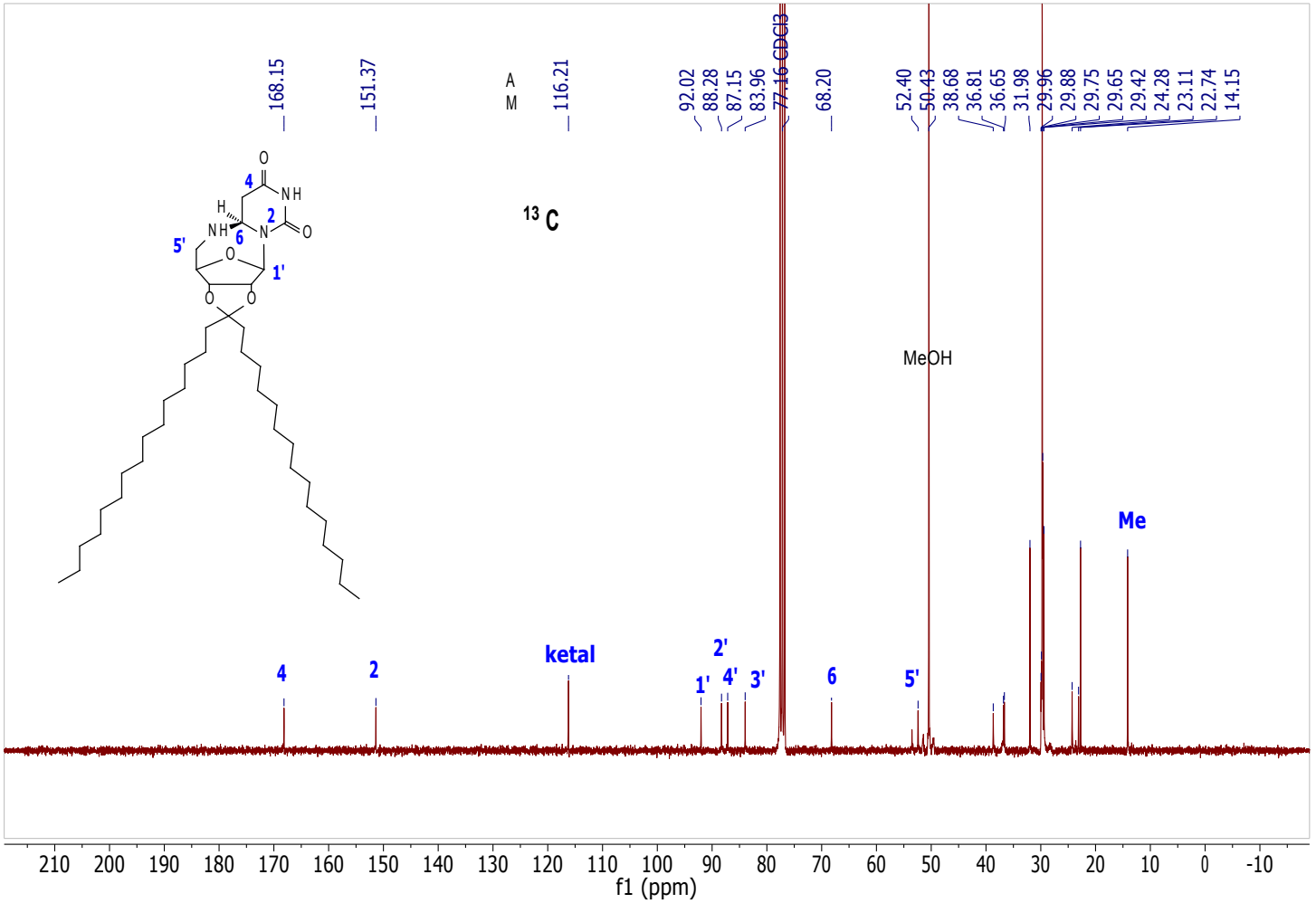

Figure S17. ^{13}C spectrum of N-cyclonucleoside (**2b**)

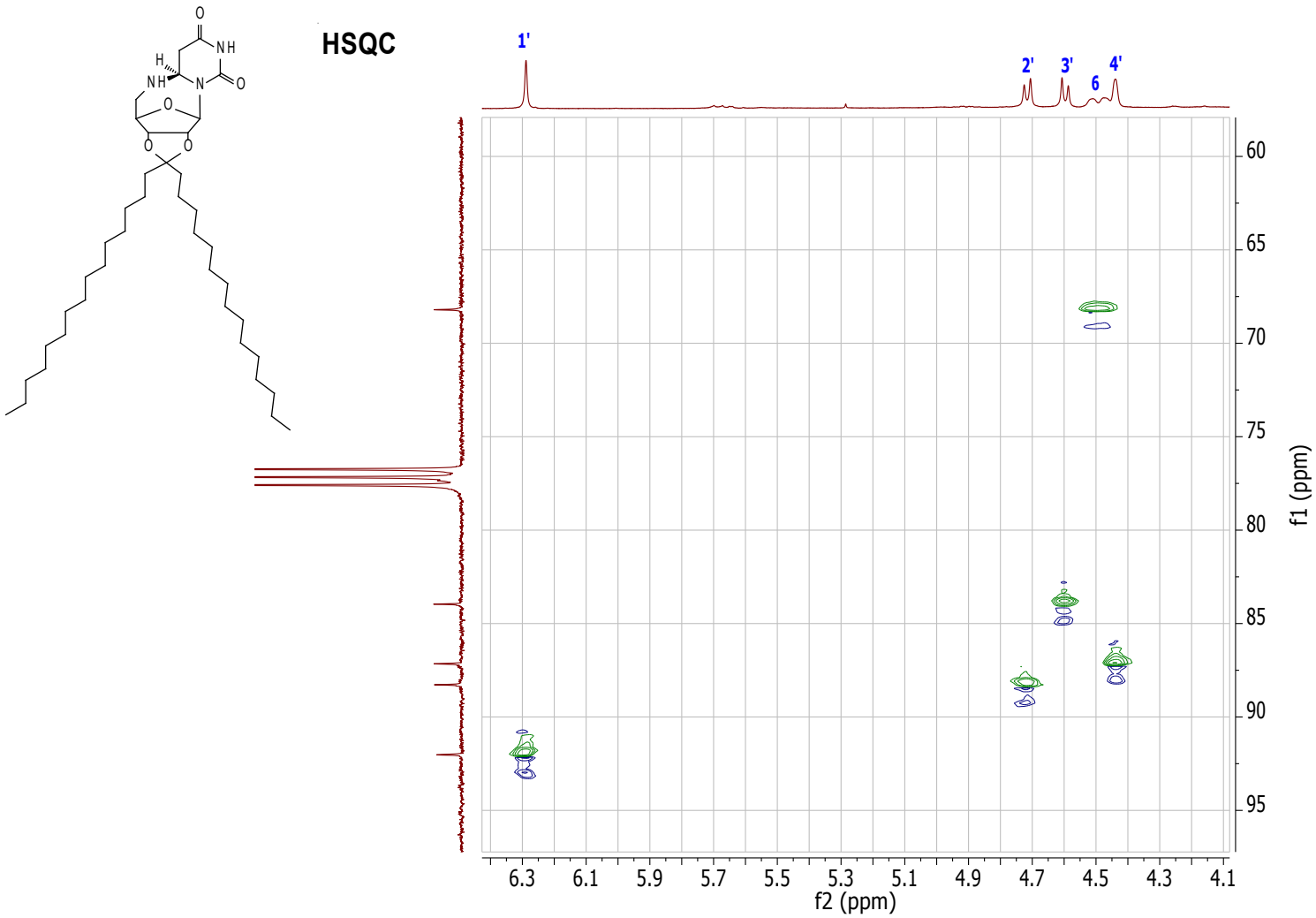

Figure S18. HSQC spectrum of N-cyclonucleoside (**2b**)

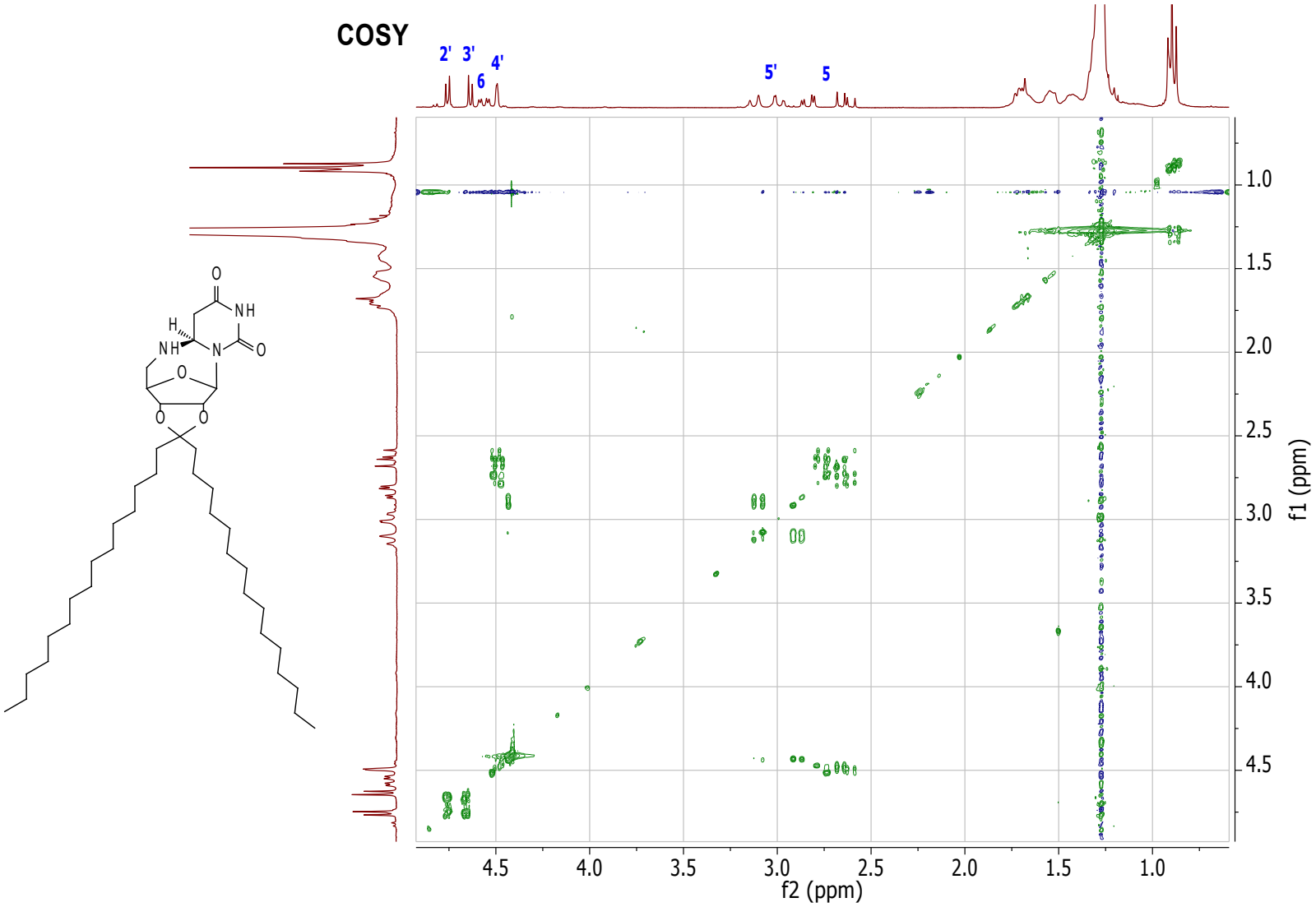

Figure S19. COSY spectrum of N-cyclonucleoside (**2b**)

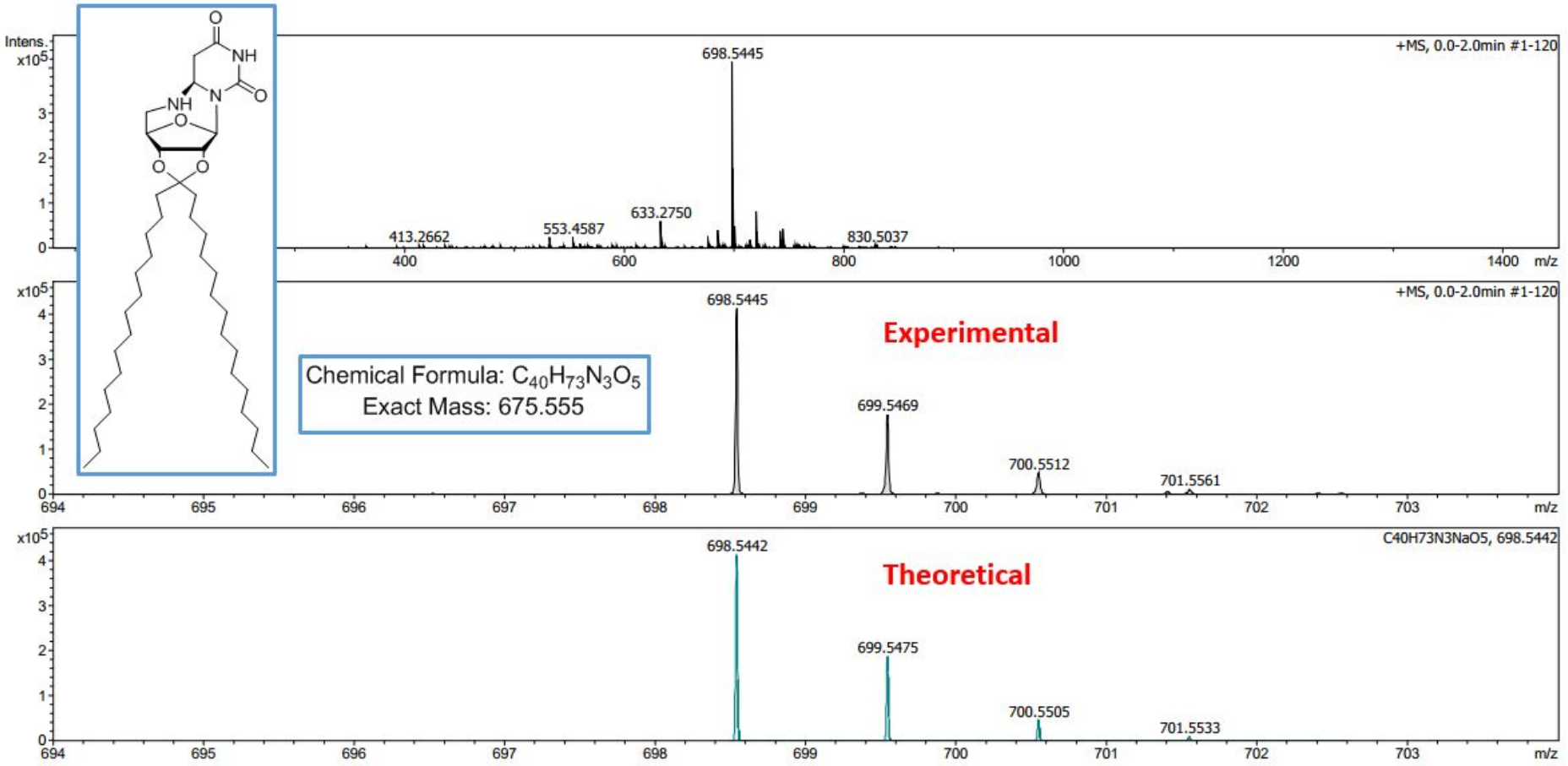

Figure S20. HRMS of N-cyclonucleoside (**2b**)

S-cyclonucleoside (**3a**)

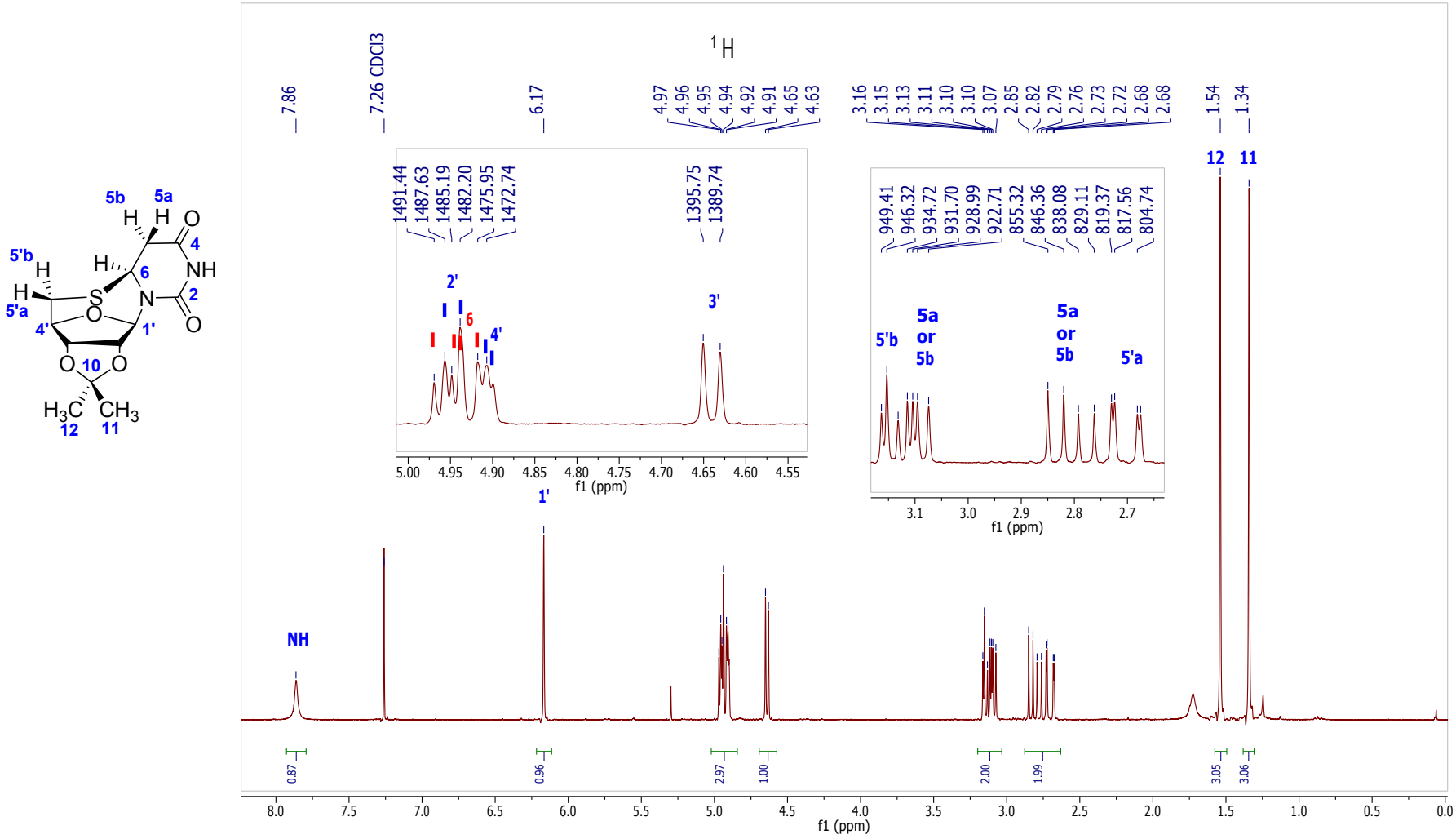

Figure S21. ^{1}H spectrum of S-cyclonucleoside (**3a**)

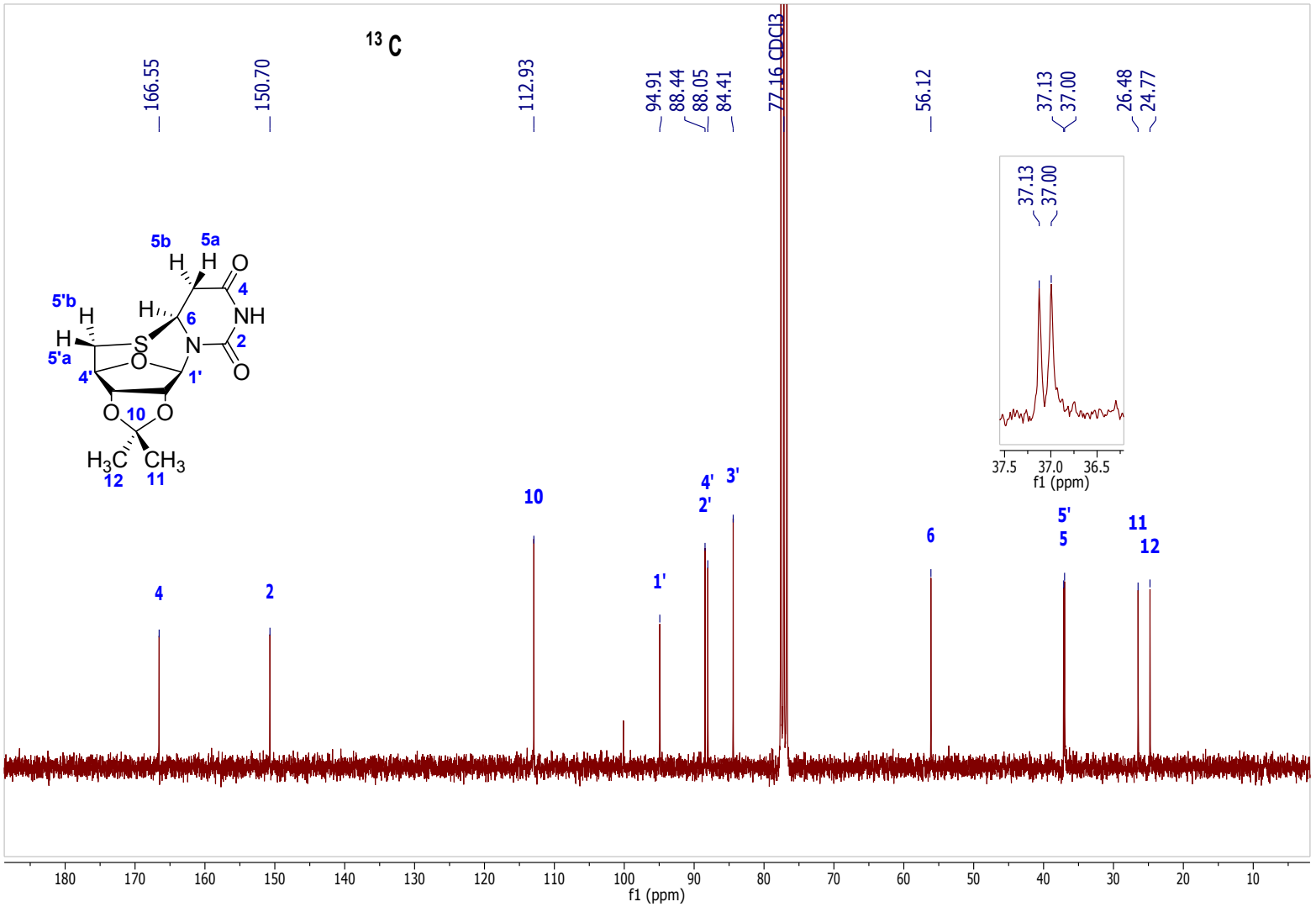

Figure S22. ^{13}C spectrum of S-cyclonucleoside (**3a**)

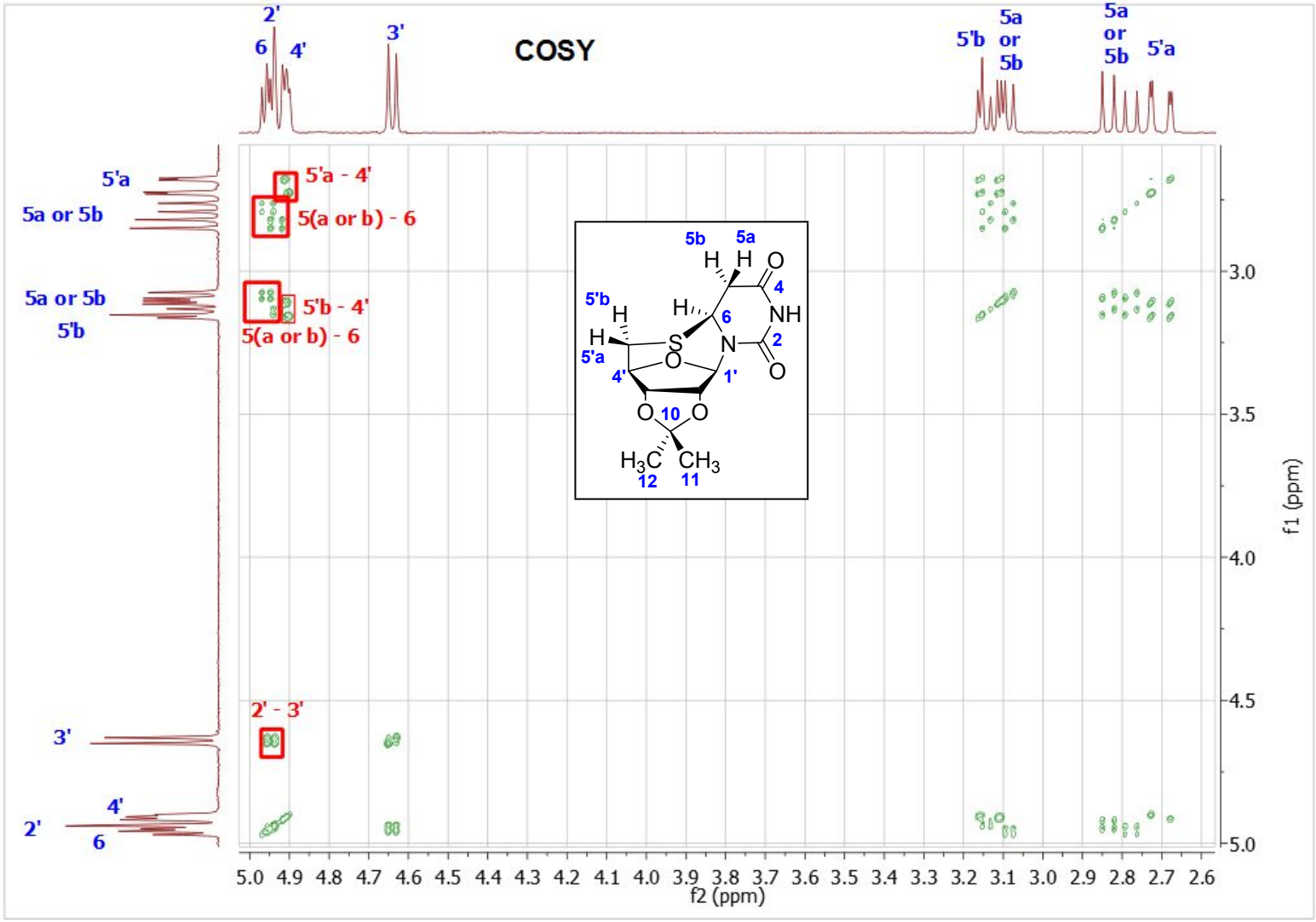

Figure S23. COSY spectrum of S-cyclonucleoside (**3a**)

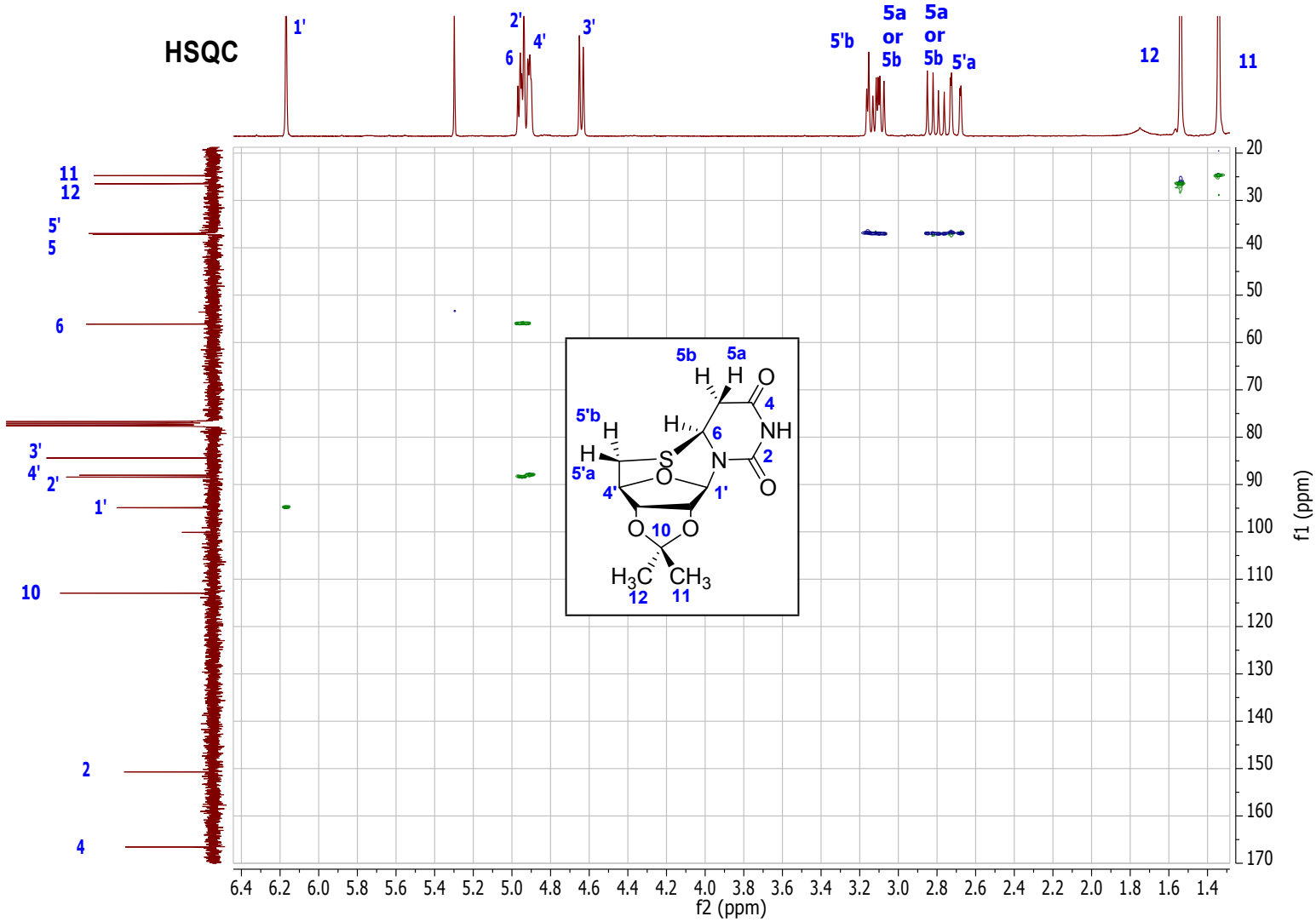

Figure S24. HSQC spectrum of S-cyclonucleoside (**3a**)

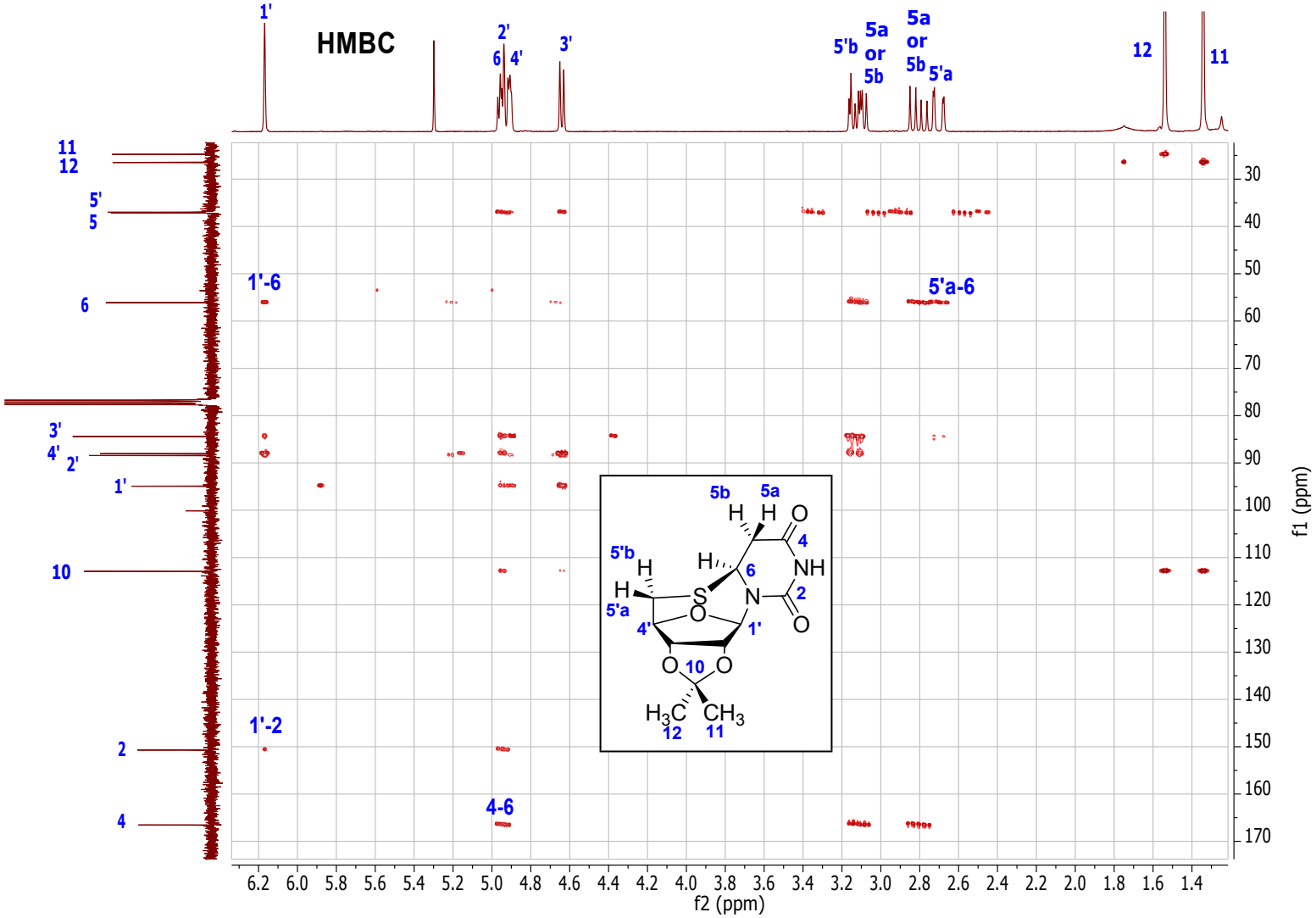

Figure S25. HMBC spectrum of S-cyclonucleoside (**3a**)

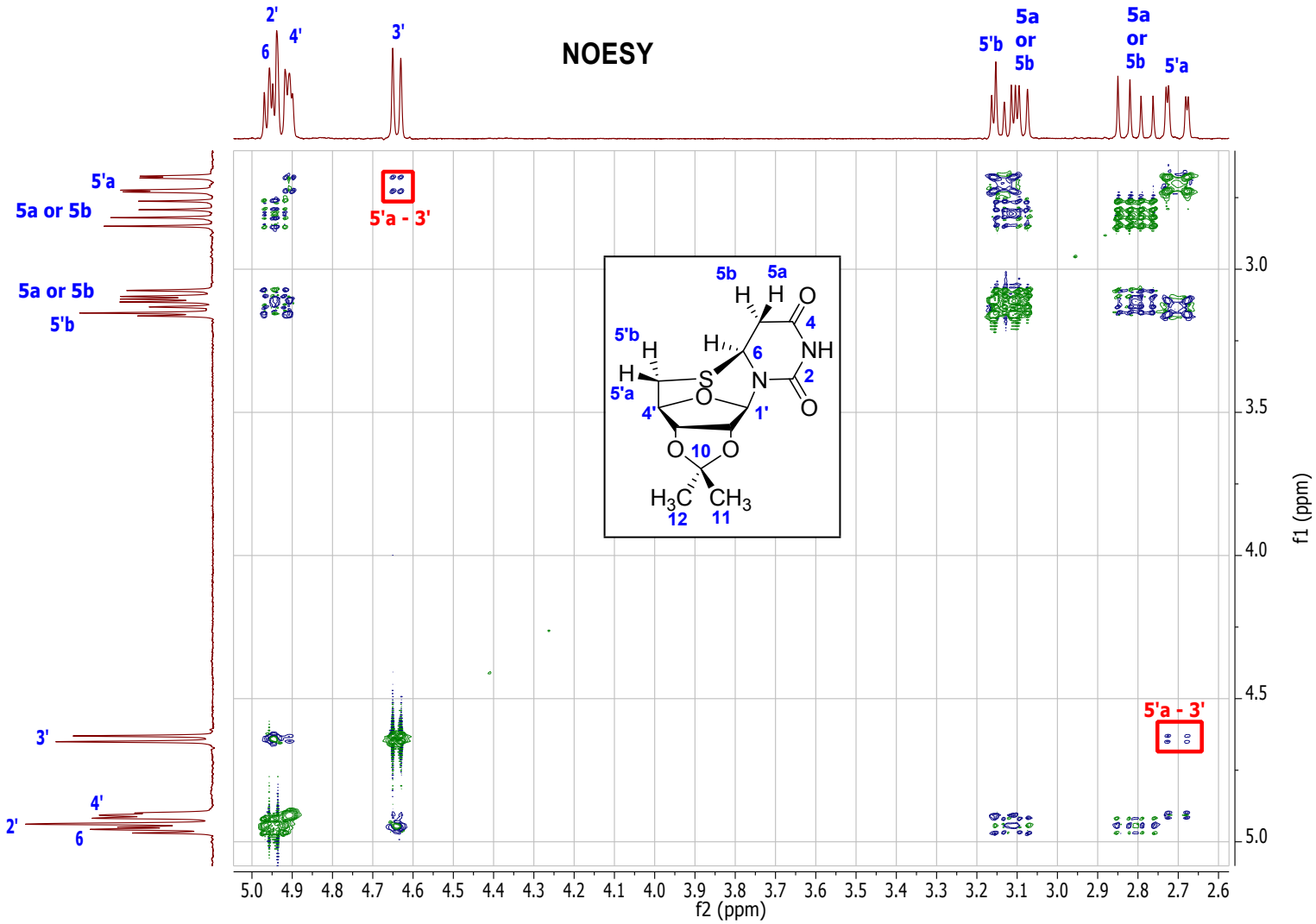

Figure S26. ROESY spectrum of S-cyclonucleoside (**3a**)

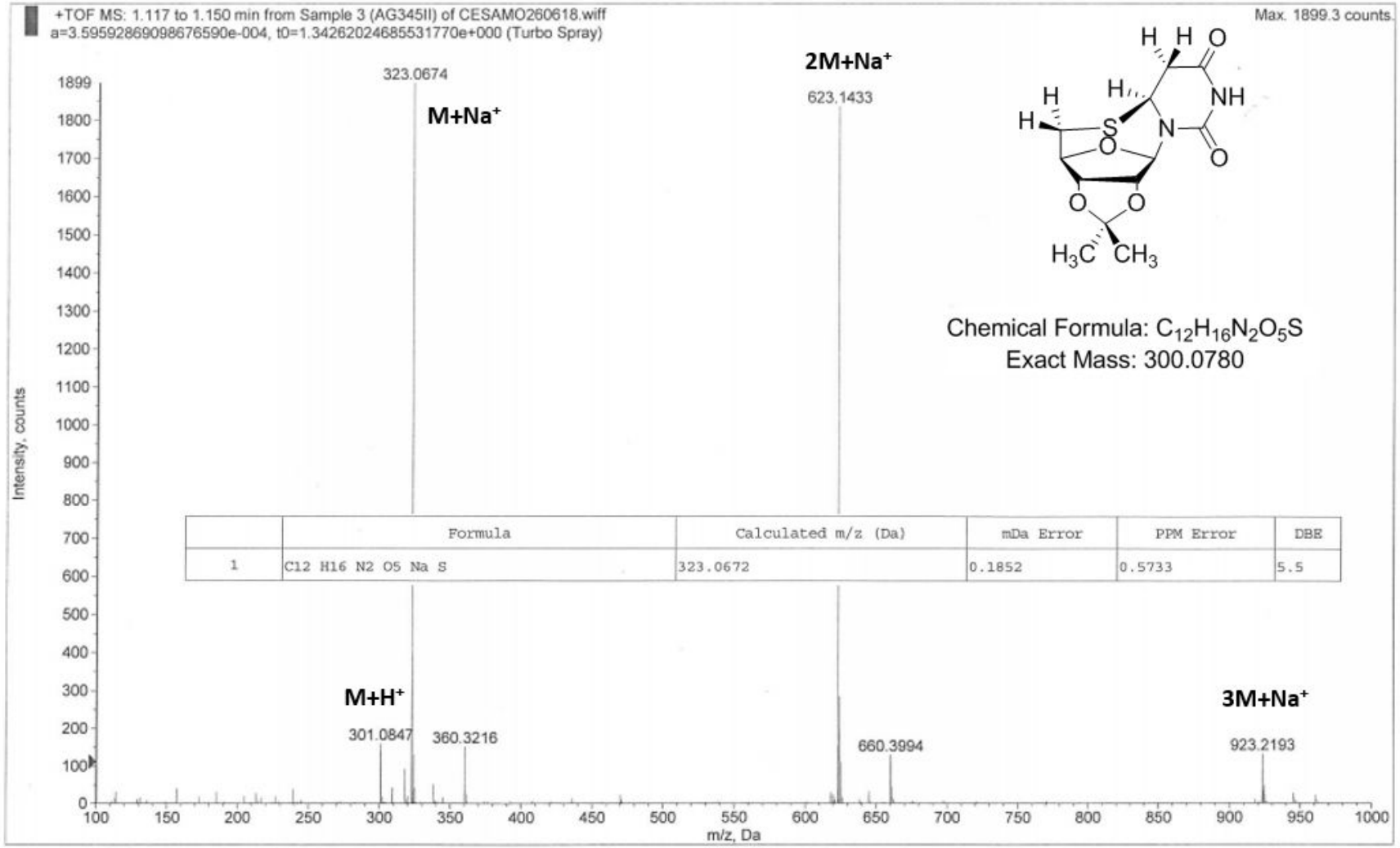

Figure S27. HRMS of S-cyclonucleoside (**3a**)

S-cyclonucleoside (**3b**)

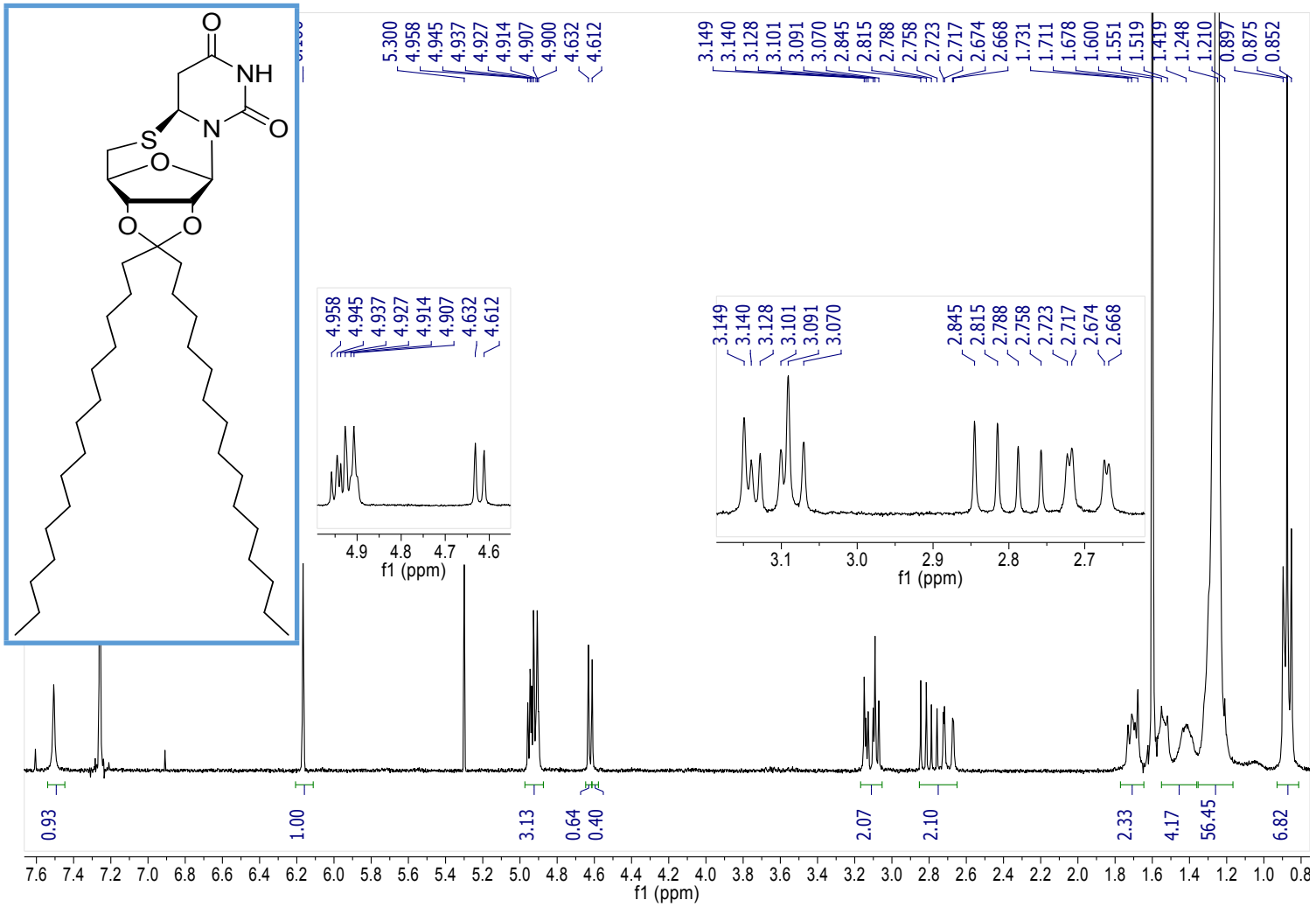

Figure S28. ^{1}H spectrum of S-cyclonucleoside (**3b**)

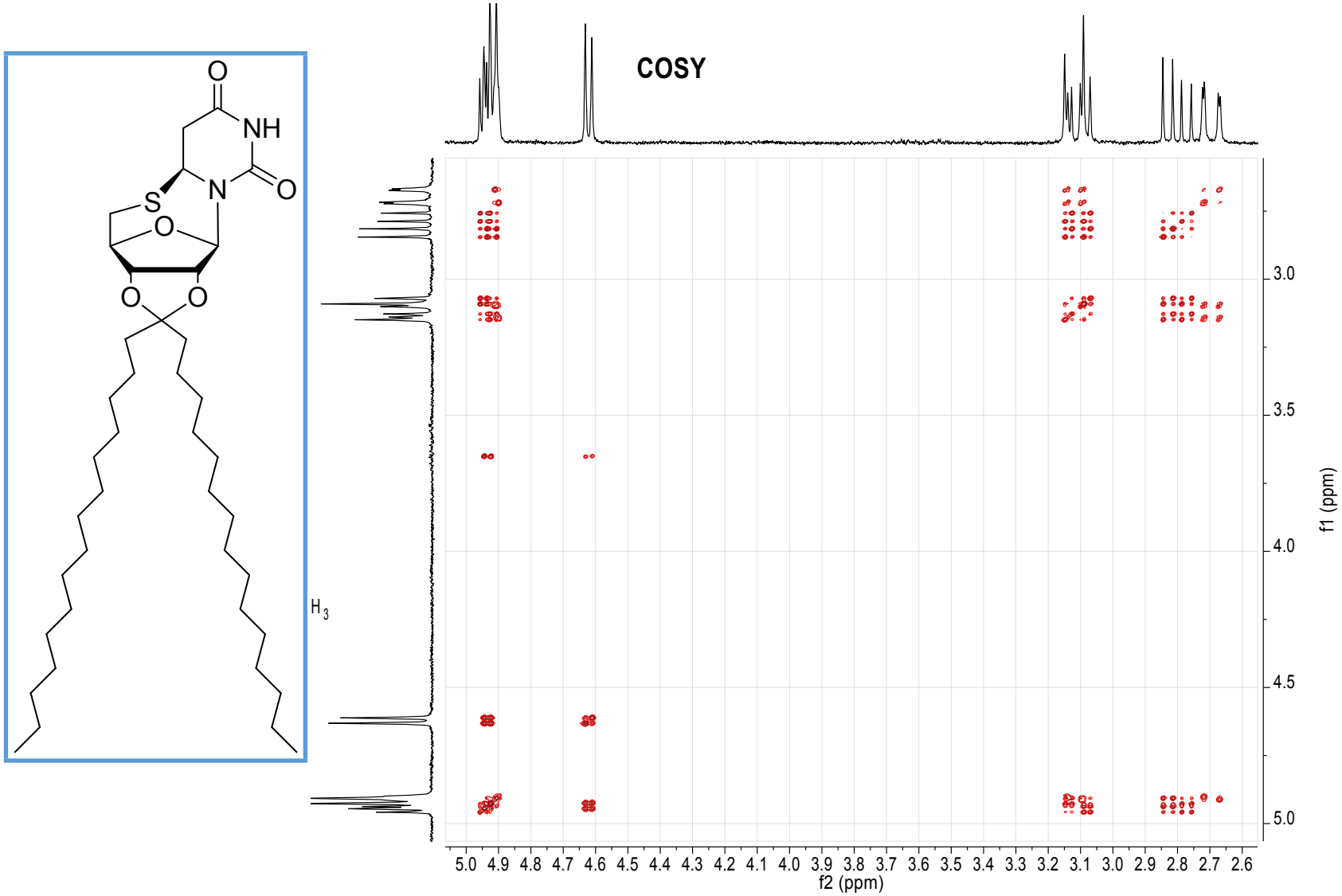

Figure S29. COSY spectrum of S-cyclonucleoside (**3b**)

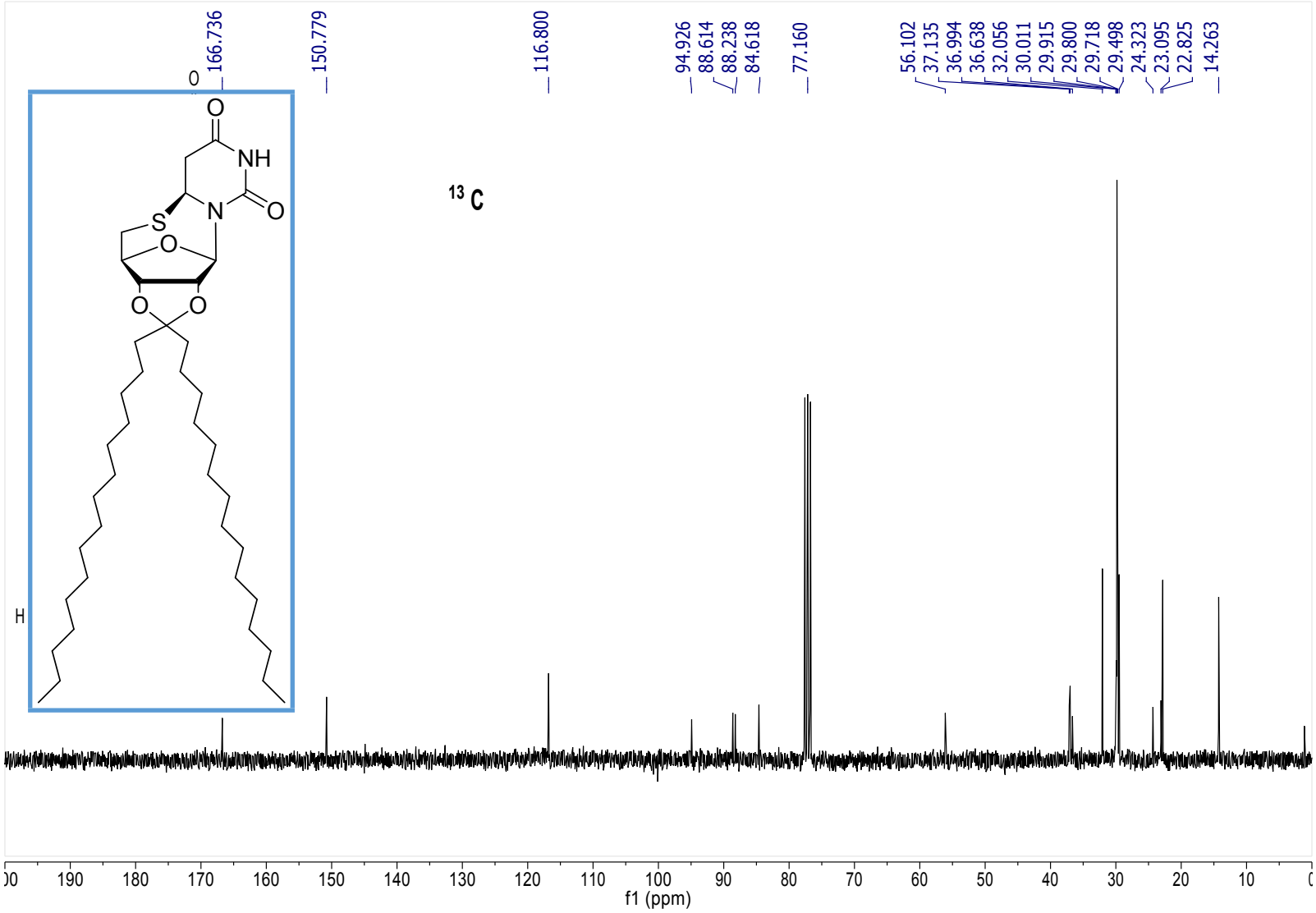

Figure S30. ^{13}C spectrum of S-cyclonucleoside (**3b**)

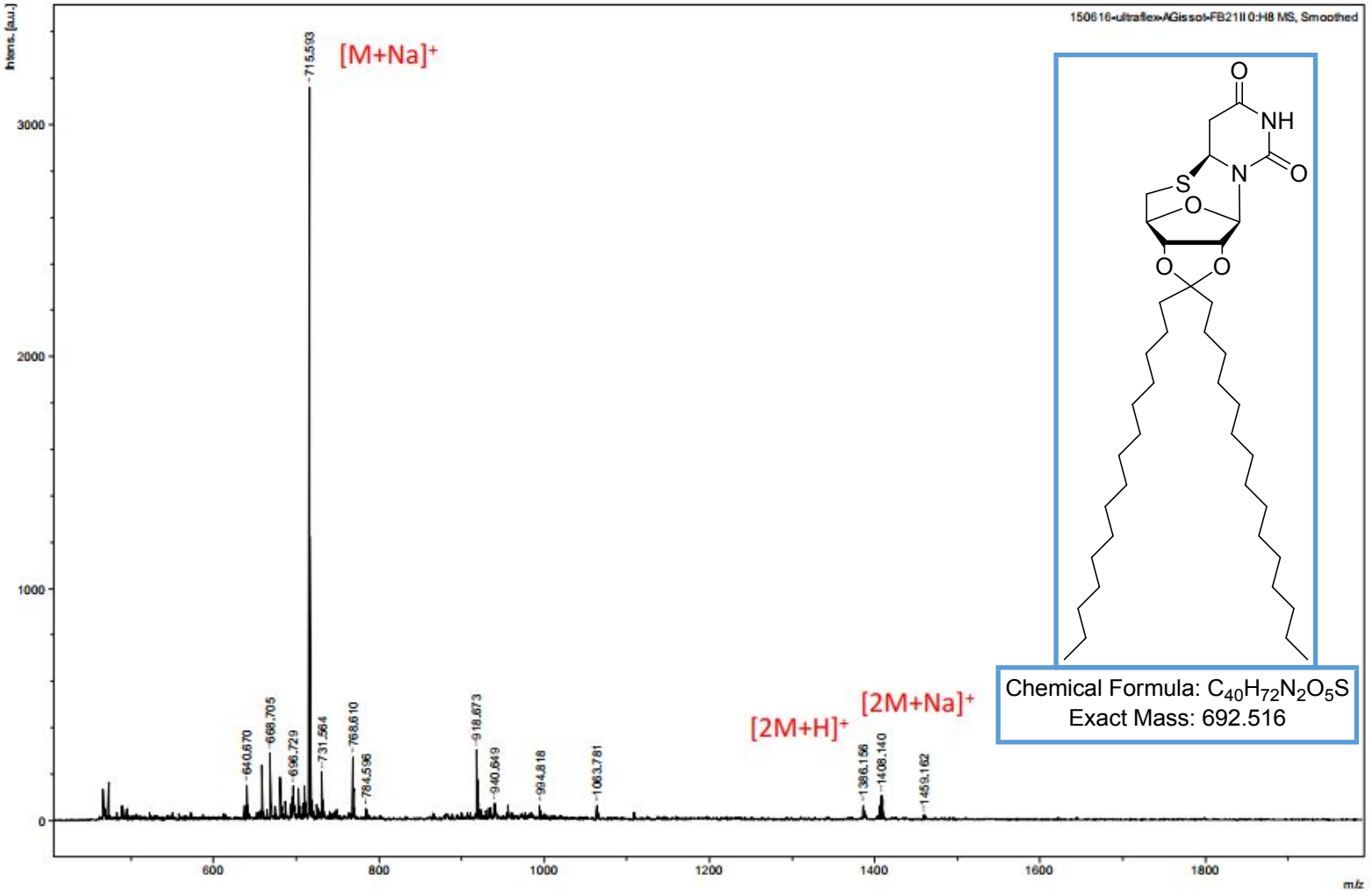

Figure S31. MS of S-cyclonucleoside (**3b**)

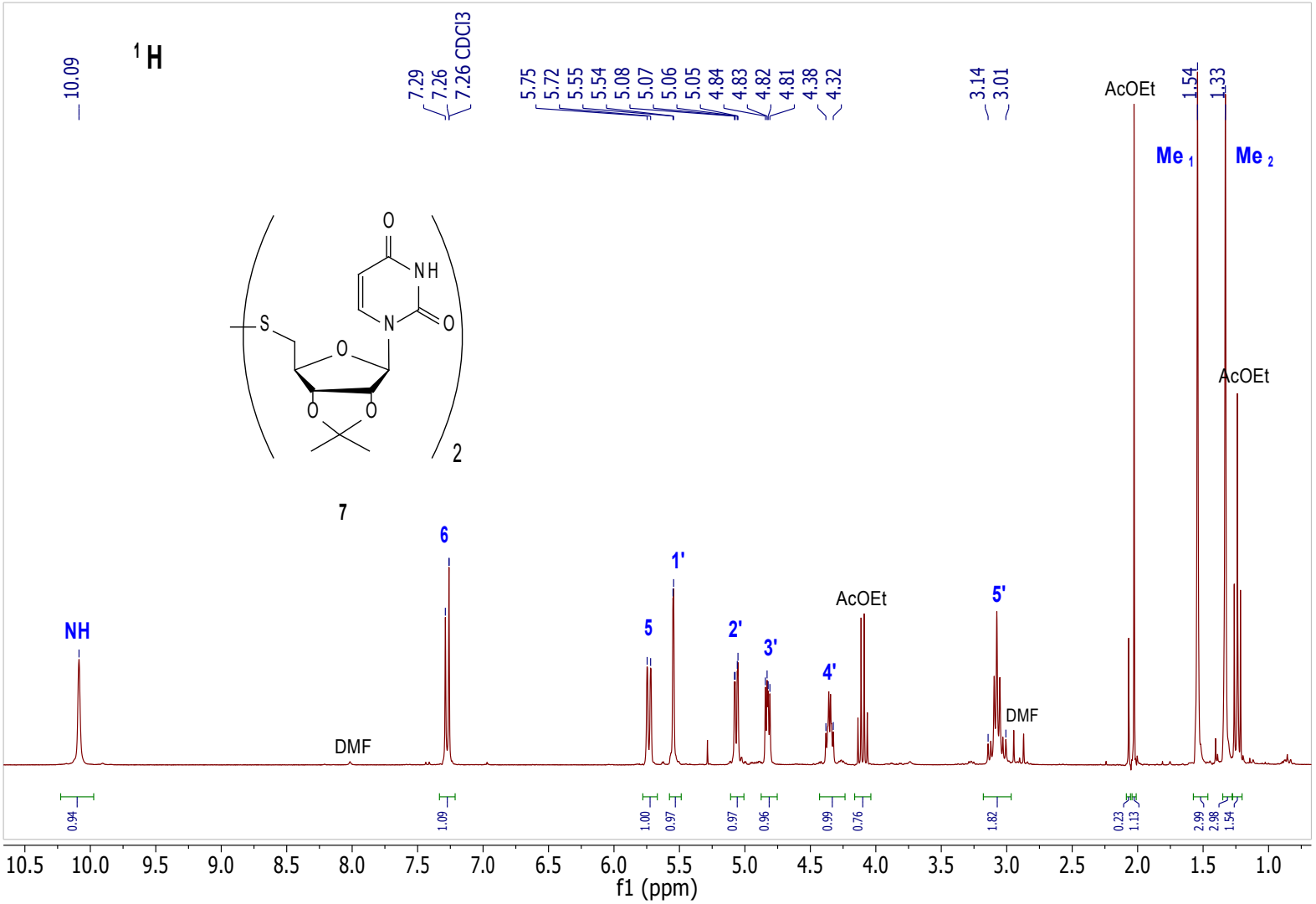

7

Figure S32. ^{1}H spectrum of the disulfide (**7**).

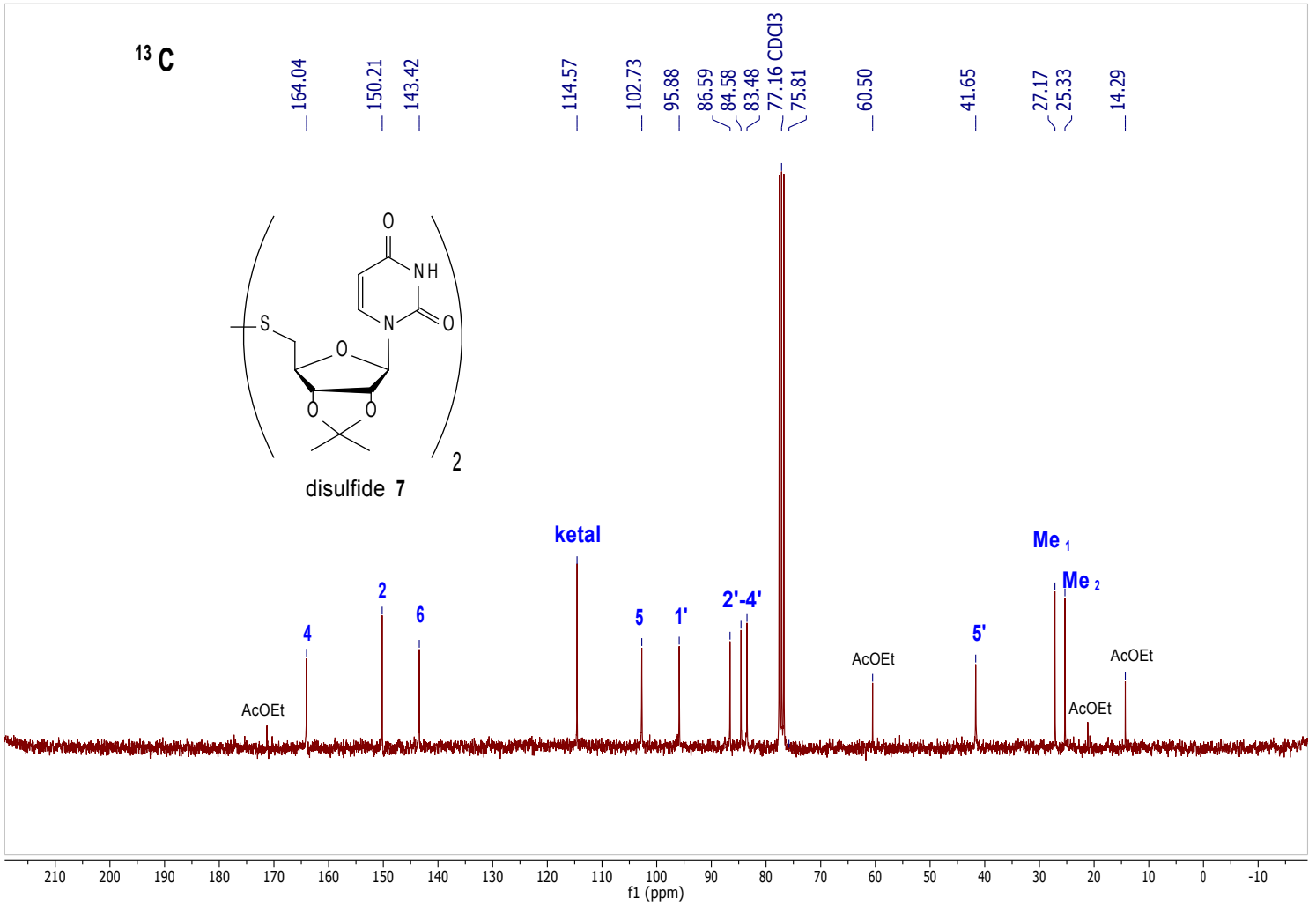

Figure S33. ^{13}C spectrum of the disulfide (**7**).

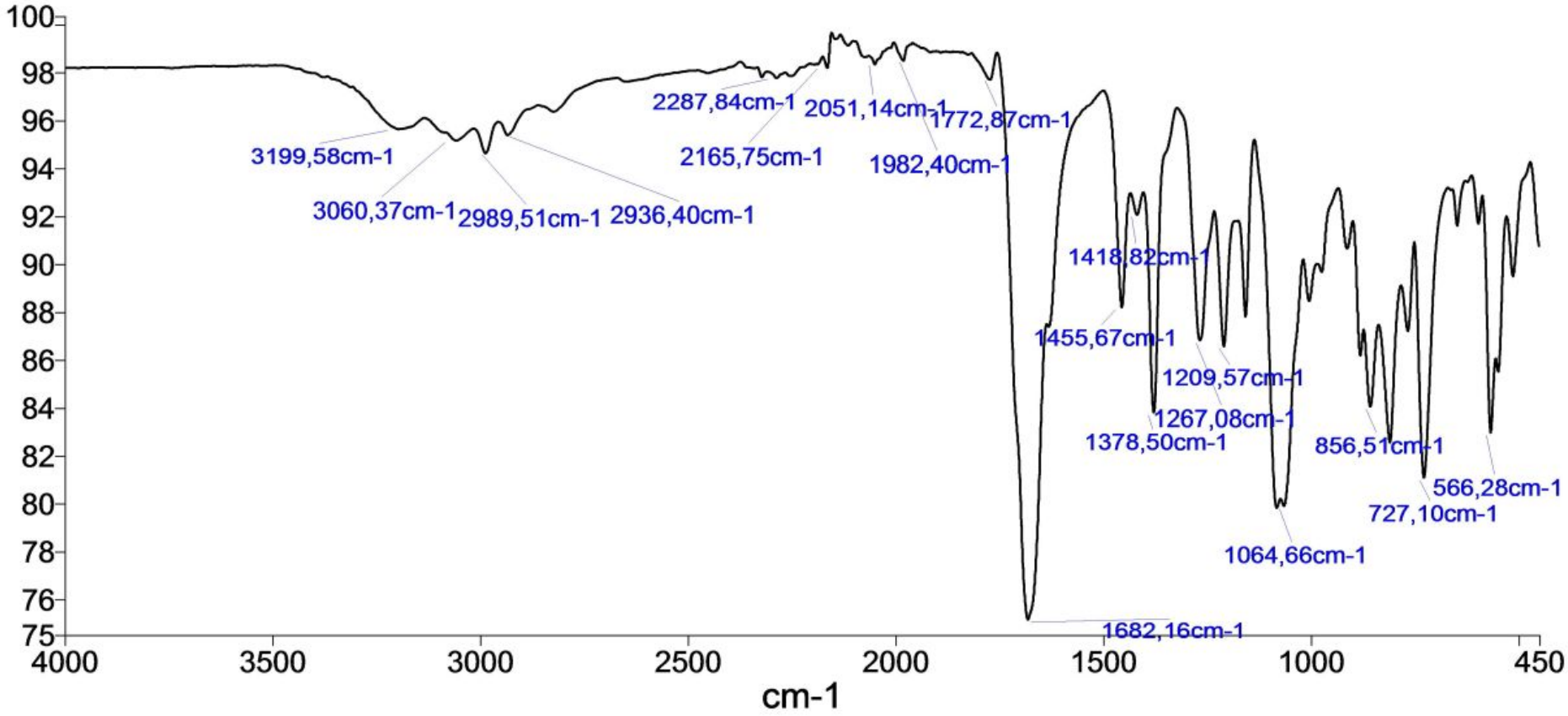

Figure S34. IR spectrum of the disulfide (**7**).

Analyses are in agreement with previously published data: cf *Carbohydrate Research*, **2007,** *342,* 9, 1151-1158

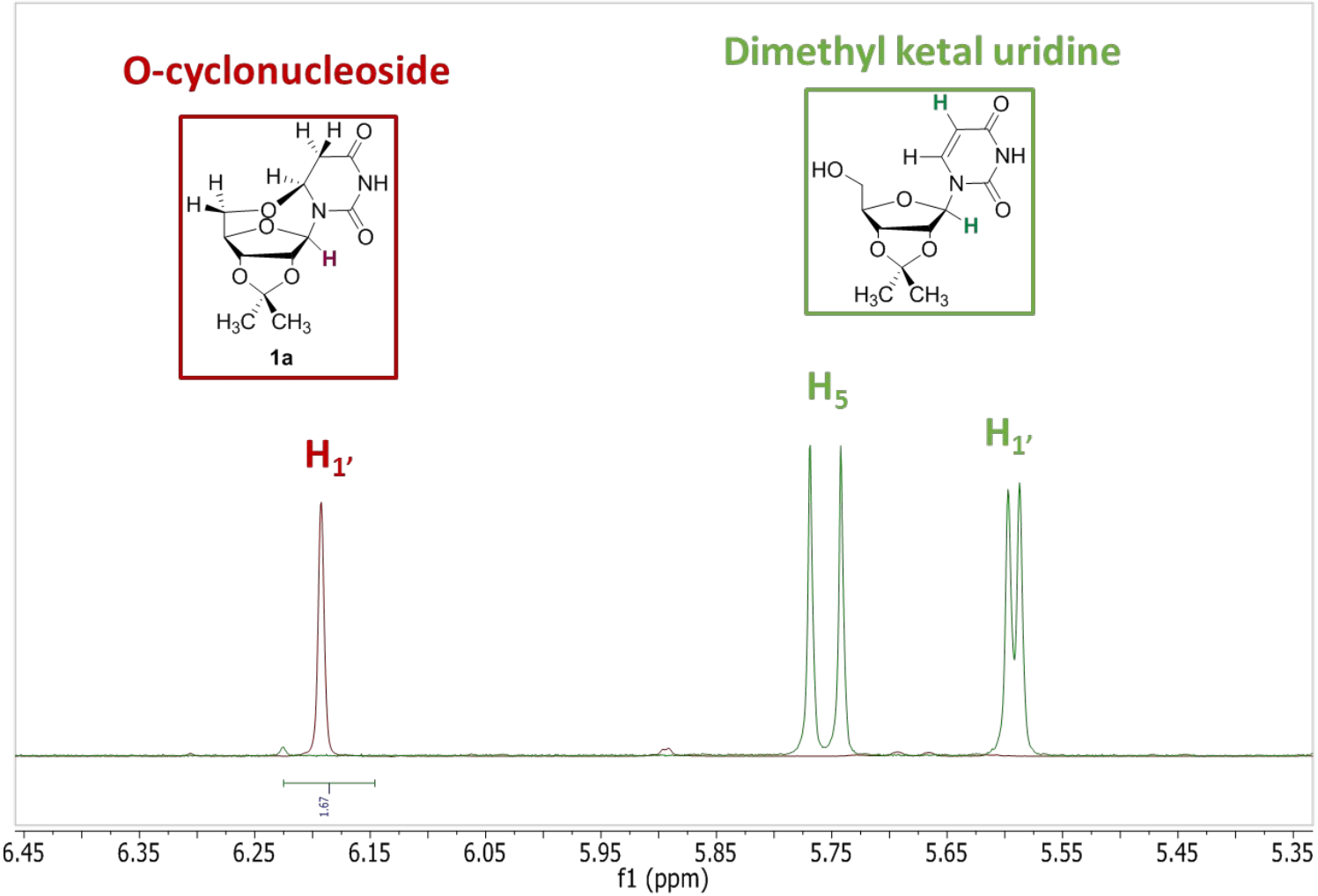

Figure S35. Comparison between the $H_{1'}$ chemical shift in dimethyl ketal uridine and O-cyclonucleoside (**1a**).

X-ray analyses were carried out[1] on a FR-X Rigaku diffractometer with rotating anode and monochromatic Cu-Kα radiation (λ= 1. 54184 Å) and a Dectris Pilatus 200K detector. Data reduction was performed with CrysAlisPro[2]. The structures were solved by direct methods and refined using Shelx 2014 suite of programs[3] in the integrated WinGX system[4]. The positions of the H atoms were deduced from coordinates of the non-H atoms and confirmed by Fourier synthesis. The non-H atoms were refined with anisotropic temperature parameters. H atoms were included for structure factor calculations but not refined. The program Mercury[5] was used for analysis and drawing figures.

[1] Crystal Clear Software, Version 2.1 43b (2013), Rigaku-MSC Corporation, Tokyo, Japan.

[2] CrysAlis PRO Software, Version 171.38.43 (2015). Rigaku Oxford Diffraction, Yarnton, England.

[3] Sheldrick, G.M., 2008, Acta Cryst. A64, 112-122.

[4] Farrugia, L.J., 1999, J. Appl. Cryst., 32, 837-838.

[5] Macrae, C. F. et al., 2008, J. Appl. Cryst., 41, 466-470.

Table S1. Crystal data and structure refinement for O-cyclonucleoside (**1**).

Identification code	ag347		Theta range for data collection	6.485 to 68.244°
Empirical formula	$C_{13}H_{17}Cl_3N_2O_6$		Index ranges	-20≤h≤18, -10≤k≤9, -13≤l≤13
Formula weight	403.63		Reflections collected	12488
Temperature	153(2) K		Independent reflections	2865 [R(int) = 0.0319]
Wavelength	1.54184 Å		Completeness to theta = 67.684°	99.6 %
Crystal system	Monoclinic		Absorption correction	Semi-empirical from equivalents
Space group	C2		Max. and min. transmission	1.00000 and 0.50543
Unit cell dimensions	a = 16.6577(3) Å	a= 90°	Refinement method	Full-matrix least-squares on F^2
	b = 9.0916(2) Å	b= 102.302(2)°	Data / restraints / parameters	2865 / 19 / 259
	c = 11.5007(2) Å	g = 90°.	Goodness-of-fit on F^2	1.014
Volume	1701.73(6) $Å^3$		Final R indices [I>2sigma(I)]	R1 = 0.0383, wR2 = 0.0992
Z	4		R indices (all data)	R1 = 0.0388, wR2 = 0.0997
Density (calculated)	1.575 Mg/m^3		Absolute structure parameter	0.014(14)
Absorption coefficient	5.188 mm^{-1}		Extinction coefficient	0.0056(4)
F(000)	832		Largest diff. peak and hole	0.277 and -0.340 $e.Å^{-3}$
Crystal size	0.120 x 0.080 x 0.080 mm^3		CCDC Number	1855250

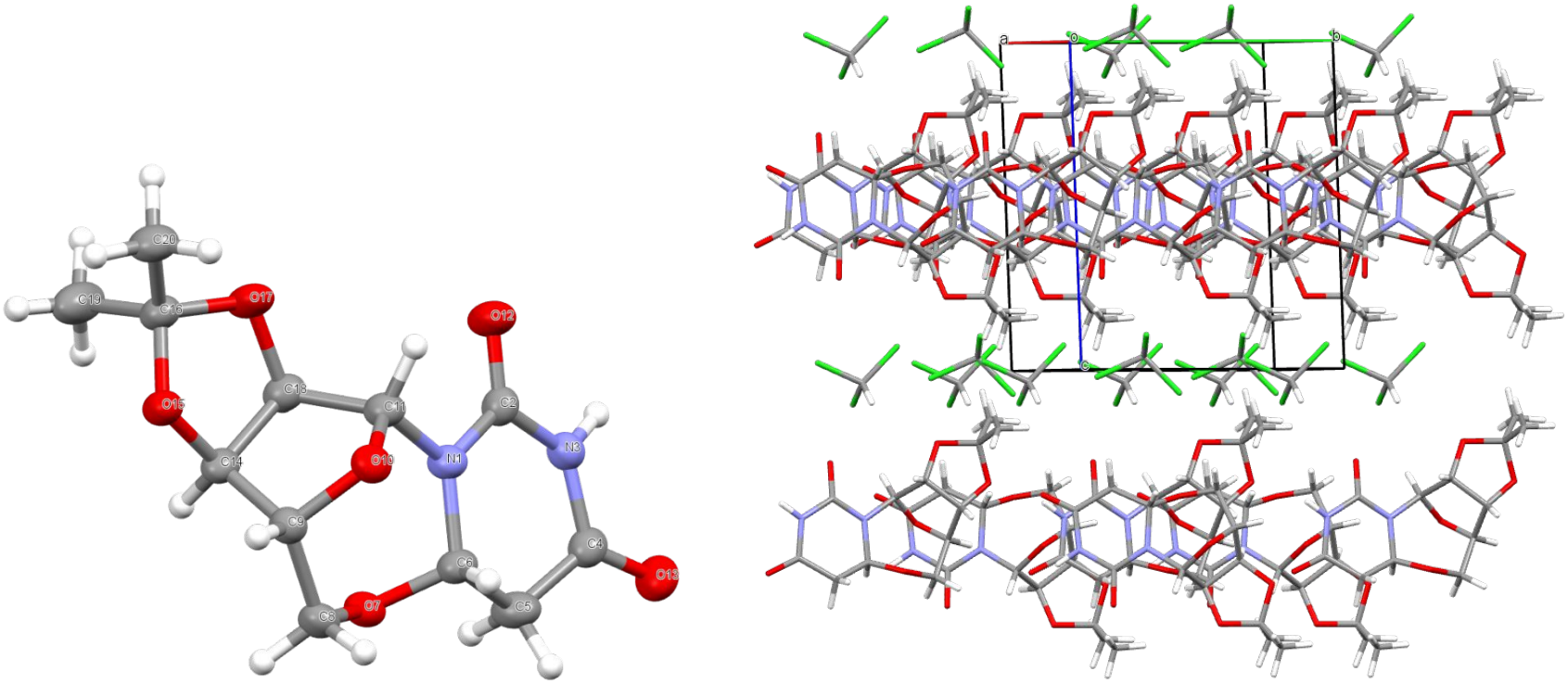

Figure of asymmetric unit of O-cyclonucleoside **1** in ellipsoid mode (left, strongly disordered chloroform has been omitted) and packing (right) showing alternative layers of compounds and solvent

Table S2. Crystal data and structure refinement for N-cyclonucleoside (**2a**).

Identification code	ag346		Theta range for data collection	4.079 to 73.788°
Empirical formula	$C_{13}H_{19}Cl_2N_3O_5$		Index ranges	-7≤h≤8, -15≤k≤18, -19≤l≤19
Formula weight	368.21		Reflections collected	24856
Temperature	100(2) K		Independent reflections	3344 [R(int) = 0.0938]
Wavelength	1.54184 Å		Completeness to theta = 67.684°	99.9 %
Crystal system	Orthorhombic		Absorption correction	Semi-empirical from equivalents
Space group	$P2_12_12_1$		Max. and min. transmission	1.00000 and 0.79125
Unit cell dimensions	a = 7.0716(3) Å	a= 90°.	Refinement method	Full-matrix least-squares on F^2
	b = 14.8200(4) Å	b= 90°.	Data / restraints / parameters	3344 / 0 / 213
	c = 15.8935(6) Å	g = 90°.	Goodness-of-fit on F^2	1.020
Volume	1665.66(10) $Å^3$		Final R indices [I>2sigma(I)]	R1 = 0.0585, wR2 = 0.1546
Z	4		R indices (all data)	R1 = 0.0609, wR2 = 0.1567
Density (calculated)	1.468 Mg/m^3		Absolute structure parameter	0.012(12)
Absorption coefficient	3.770 mm^{-1}		Extinction coefficient	n/a
F(000)	768		Largest diff. peak and hole	0.688 and -0.546 e.$Å^{-3}$
Crystal size	0.080 x 0.060 x 0.020 mm^3		CCDC Number	1855251

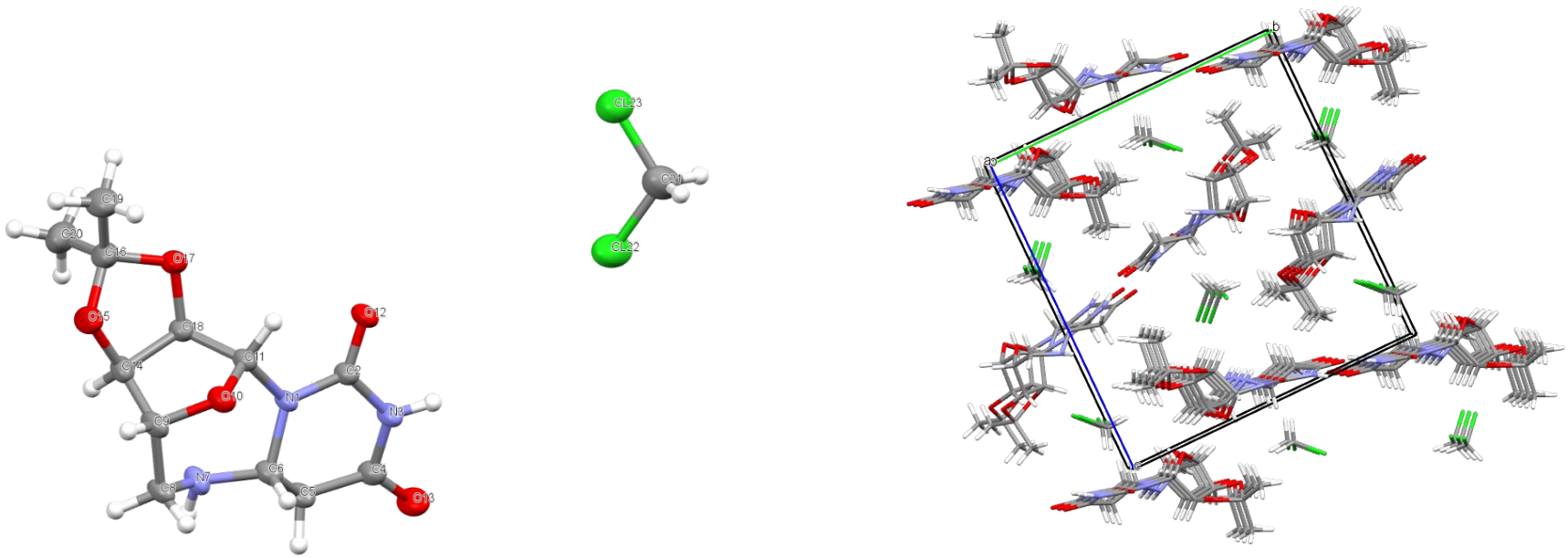

Figure of asymmetric unit of N-cyclonucleoside **2a** in ellipsoid mode (left) and packing (right) showing solvent channels

Table S3. Crystal data and structure refinement for S-cyclonucleoside (**3a**).

Identification code	ag348		Theta range for data collection	4.077 to 73.356°
Empirical formula	$C_{24}H_{32}N_4O_{10}S_2$		Index ranges	-5≤h≤6, -13≤k≤13, -14≤l≤14
Formula weight	600.65		Reflections collected	16635
Temperature	100(2) K		Independent reflections	4671 [R(int) = 0.0239]
Wavelength	1.54184 Å		Completeness to theta = 67.684°	99.2 %
Crystal system	Triclinic		Absorption correction	Semi-empirical from equivalents
Space group	P1		Max. and min. transmission	1.00000 and 0.91588
Unit cell dimensions	a = 5.6074(2) Å	a= 70.359(3)°	Refinement method	Full-matrix least-squares on F^2
	b = 10.9990(4) Å	b= 87.896(3)°	Data / restraints / parameters	4671 / 3 / 361
	c = 11.5162(4) Å	g = 80.916(3)°	Goodness-of-fit on F^2	1.029
Volume	660.45(4) $Å^3$		Final R indices [I>2sigma(I)]	R1 = 0.0343, wR2 = 0.0943
Z	1		R indices (all data)	R1 = 0.0345, wR2 = 0.0945
Density (calculated)	1.510 Mg/m^3		Absolute structure parameter	0.001 (8)
Absorption coefficient	2.400 mm^{-1}		Extinction coefficient	n/a
F(000)	316		Largest diff. peak and hole	0.538 and -0.295 e.$Å^{-3}$
Crystal size	0.100 x 0.040 x 0.030 mm^3		CCDC Number	1855252

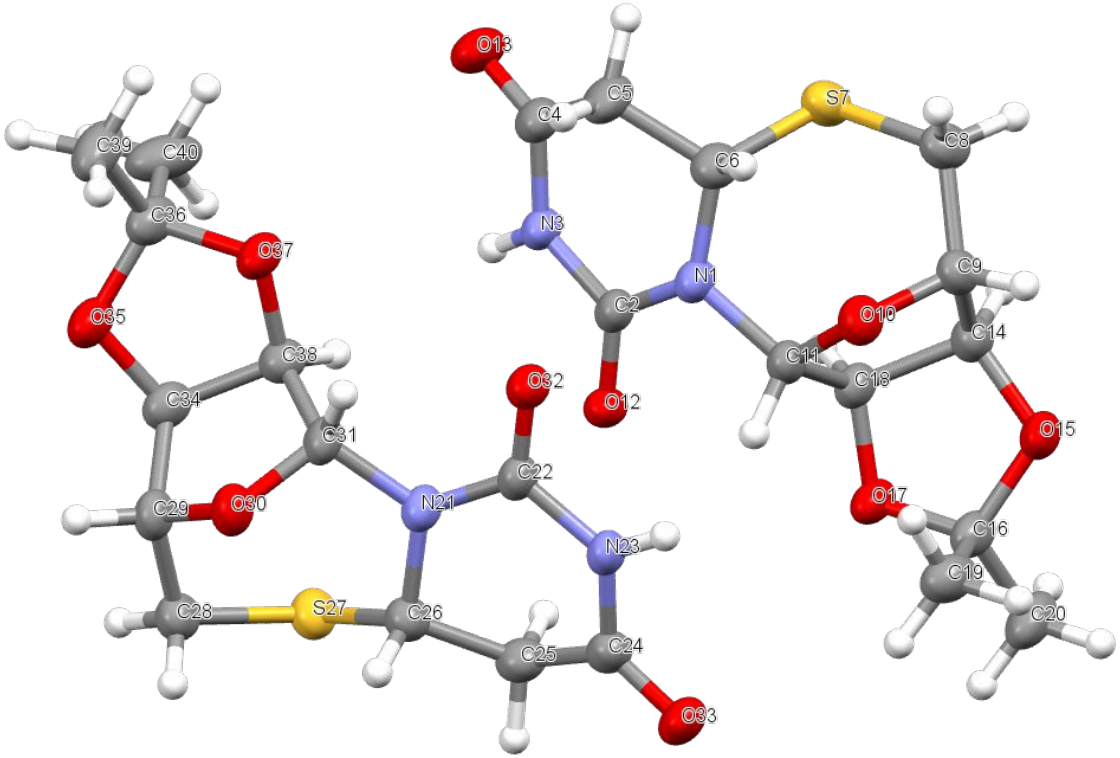

Figure of asymmetric unit of S-cyclonucleoside **3a** in ellipsoid mode

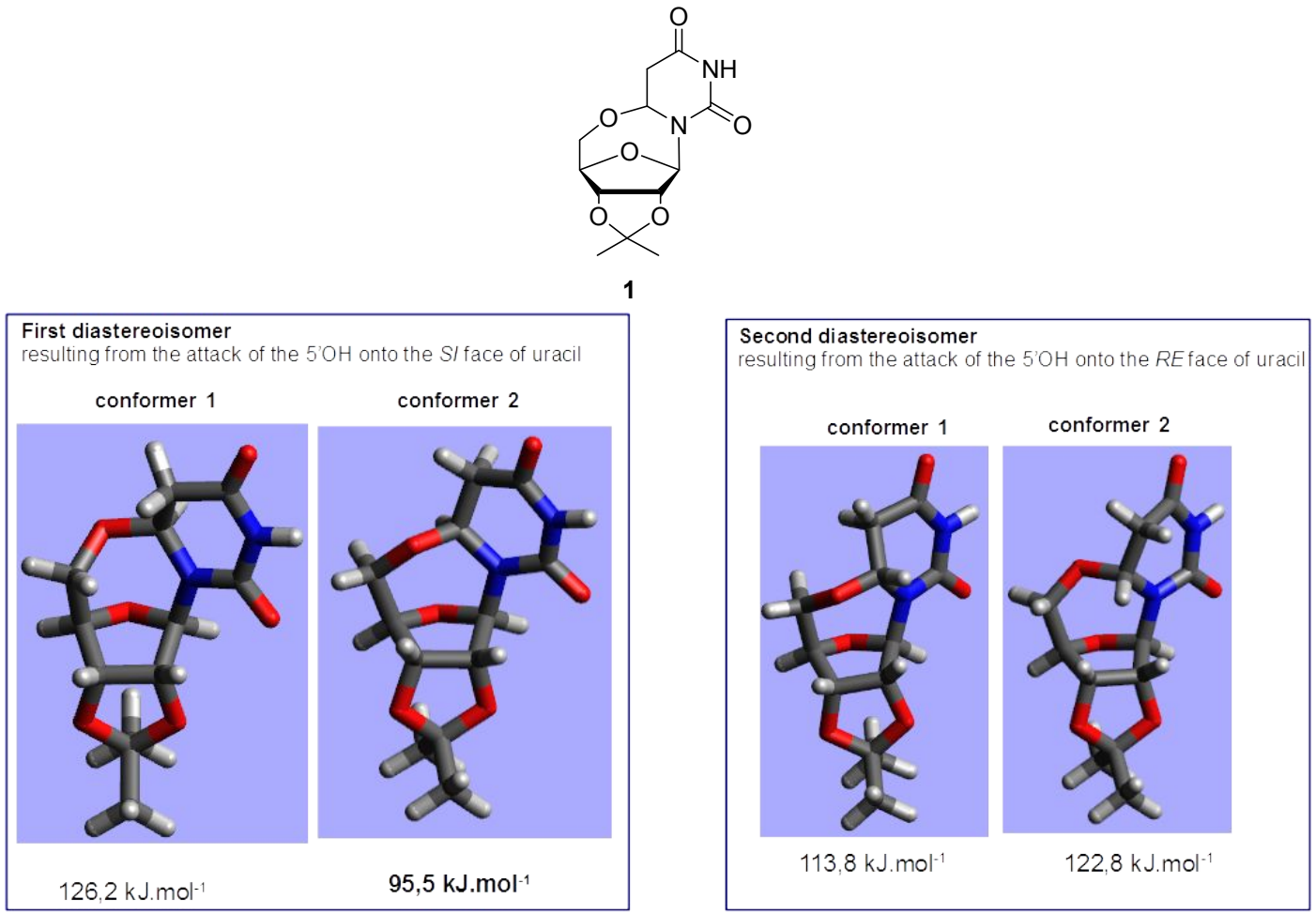

Figure S36. Energy-minimized structures for the different diastereoisomers/conformers of O-cyclonucleoside (**1**)

AMBER force field, steepest gradient

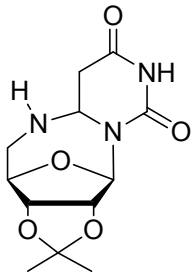

2a

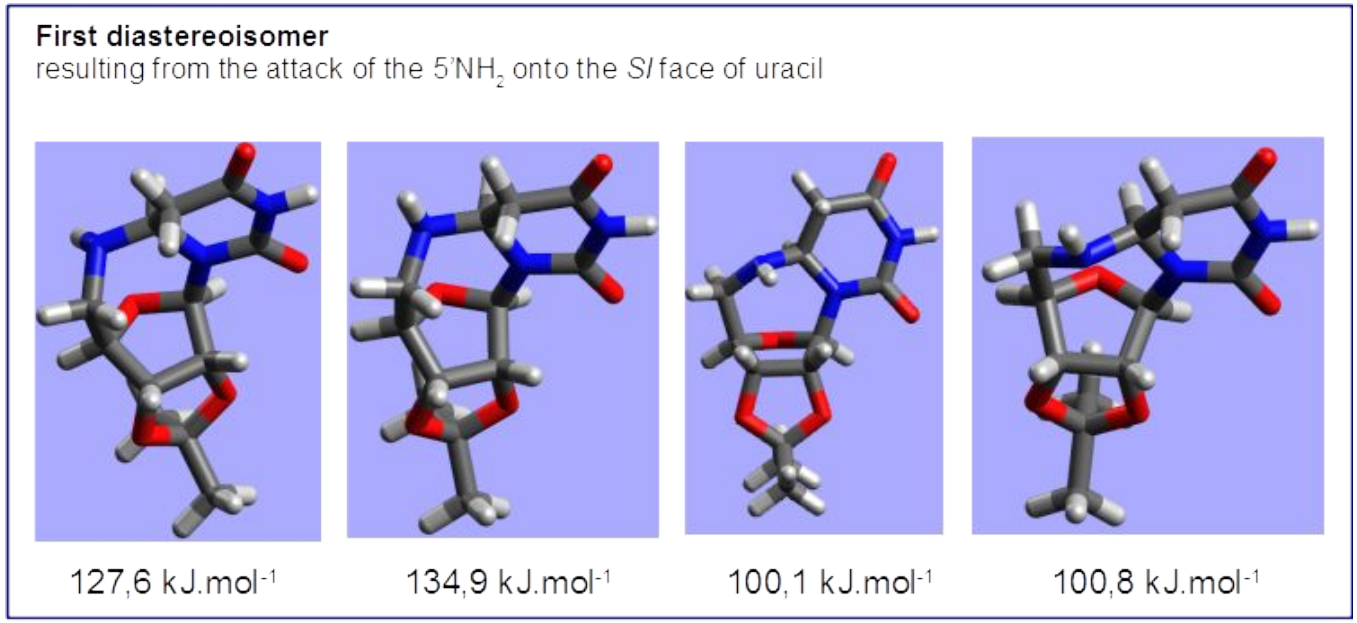

Figure S37. Energy-minimized structures for the different diastereoisomers/conformers of N-cyclonucleoside (**2a**)

AMBER force field, steepest gradient

Remark: only the diastereoisomer resulting from the attack of the 5'-NH_2 is shown as the other diastereoisomer is not favored. Each conformer is represented with the two possible configurations of the cyclized NH.

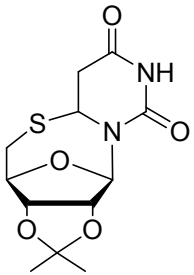

3a

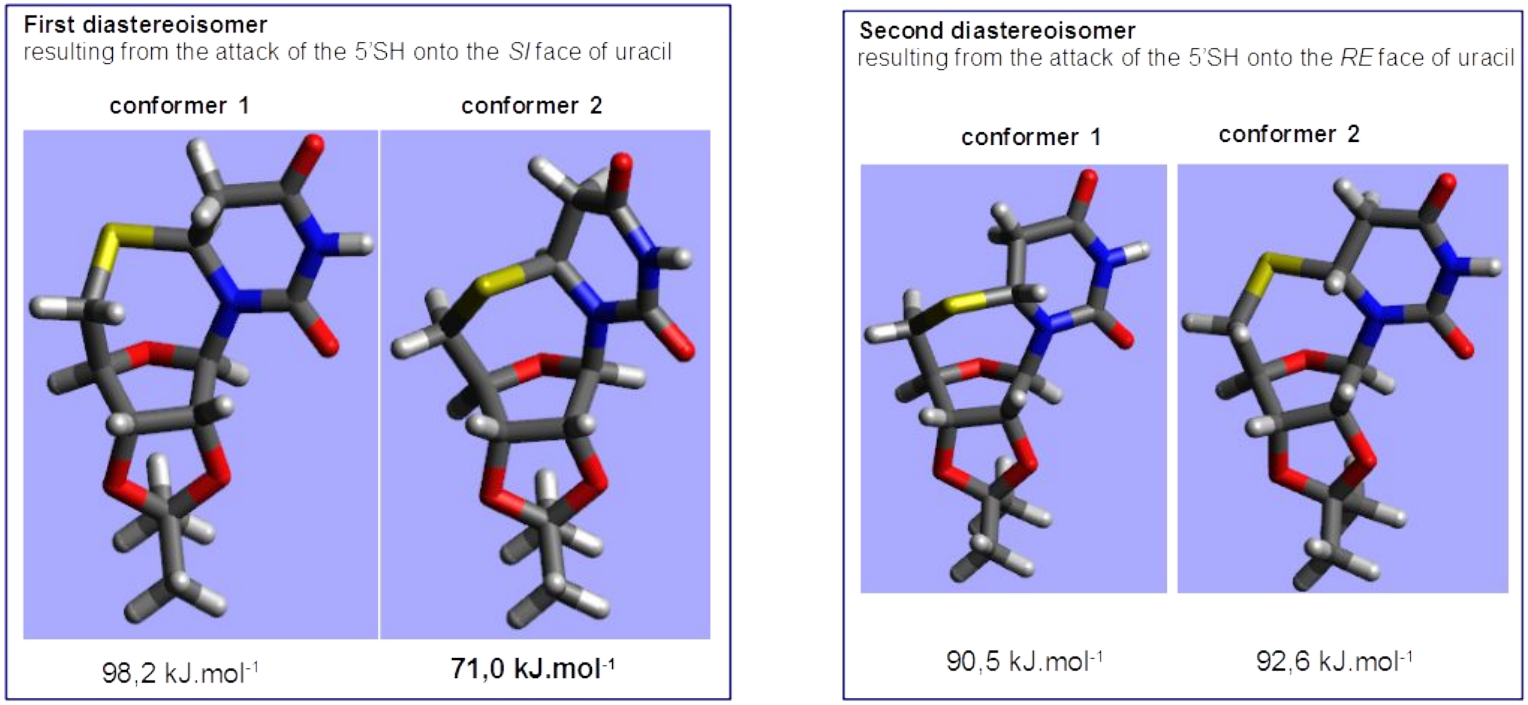

Figure S38. Energy-minimized structures for the different diastereoisomers/conformers of S-cyclonucleoside (**3a**)

AMBER force field, steepest gradient

Unprotected Uridine :

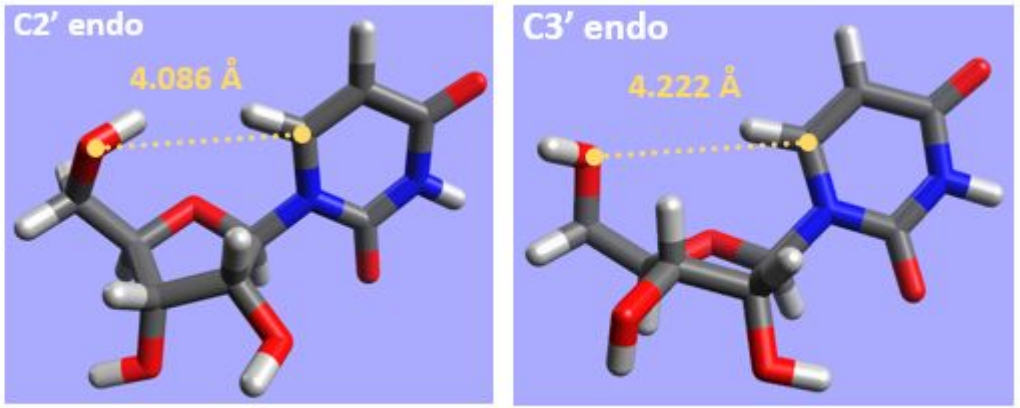

Dimethyl ketal Uridine :

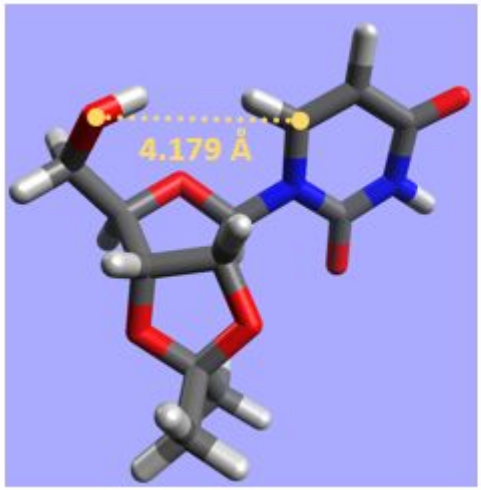

Figure S39 : Minimum distances between the 5'OH and C6 in Uridine and dimethyl ketal uridine.

Energy minimized structures, AMBER force field, and steepest gradient

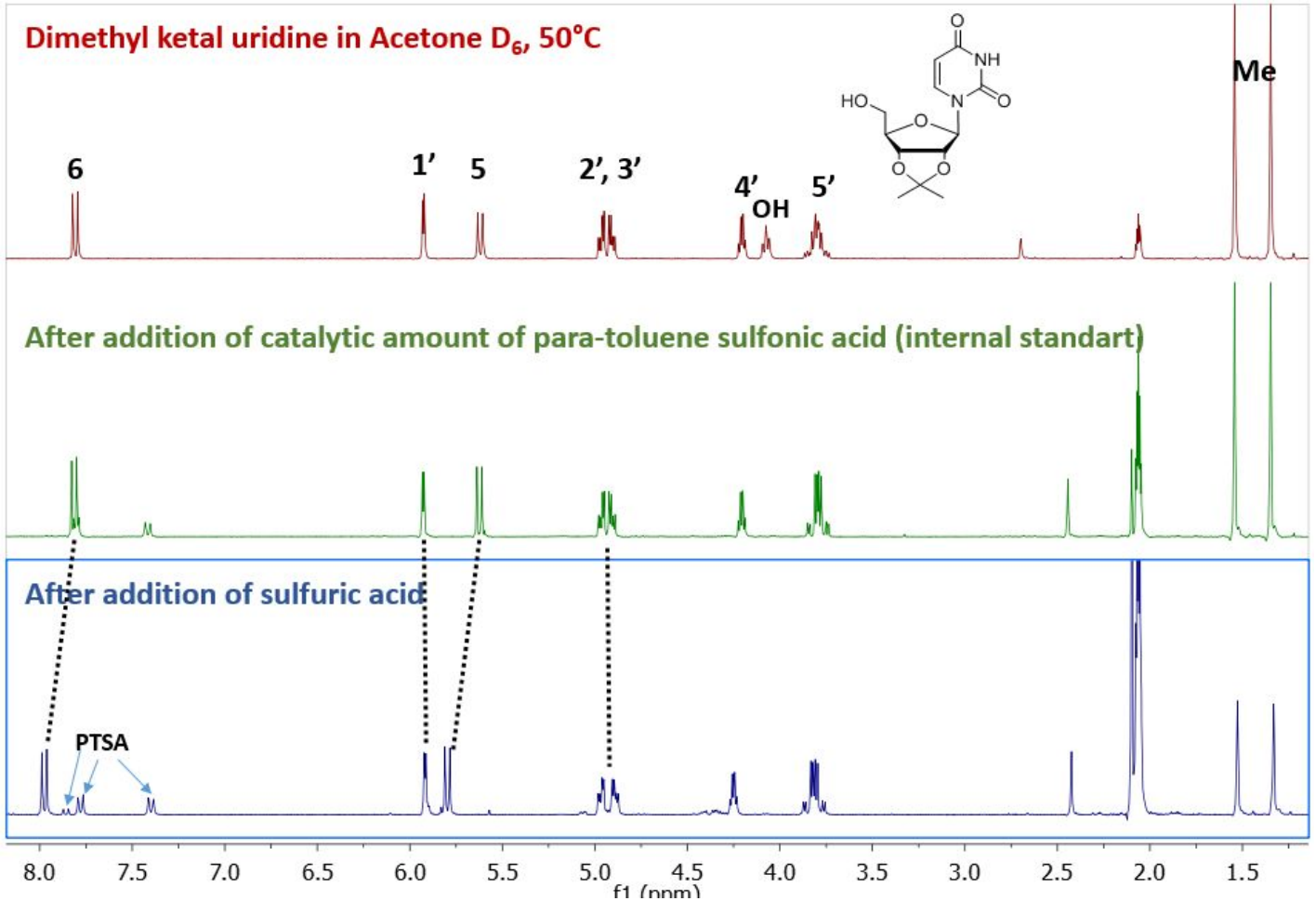

Figure S40 : NMR course of dimethyl ketal uridine in acetone D_6 before and after addition of sulfuric acid.

Addition of sulfuric acid induces the deshielding of uracil protons H_5 and H_6 most probably as a result of carbonyl protonation at C_4. One can also observe the rapid ketal exchange with acetone D_6 that takes place as evidenced by the decrease in the integration of the methyl peaks.

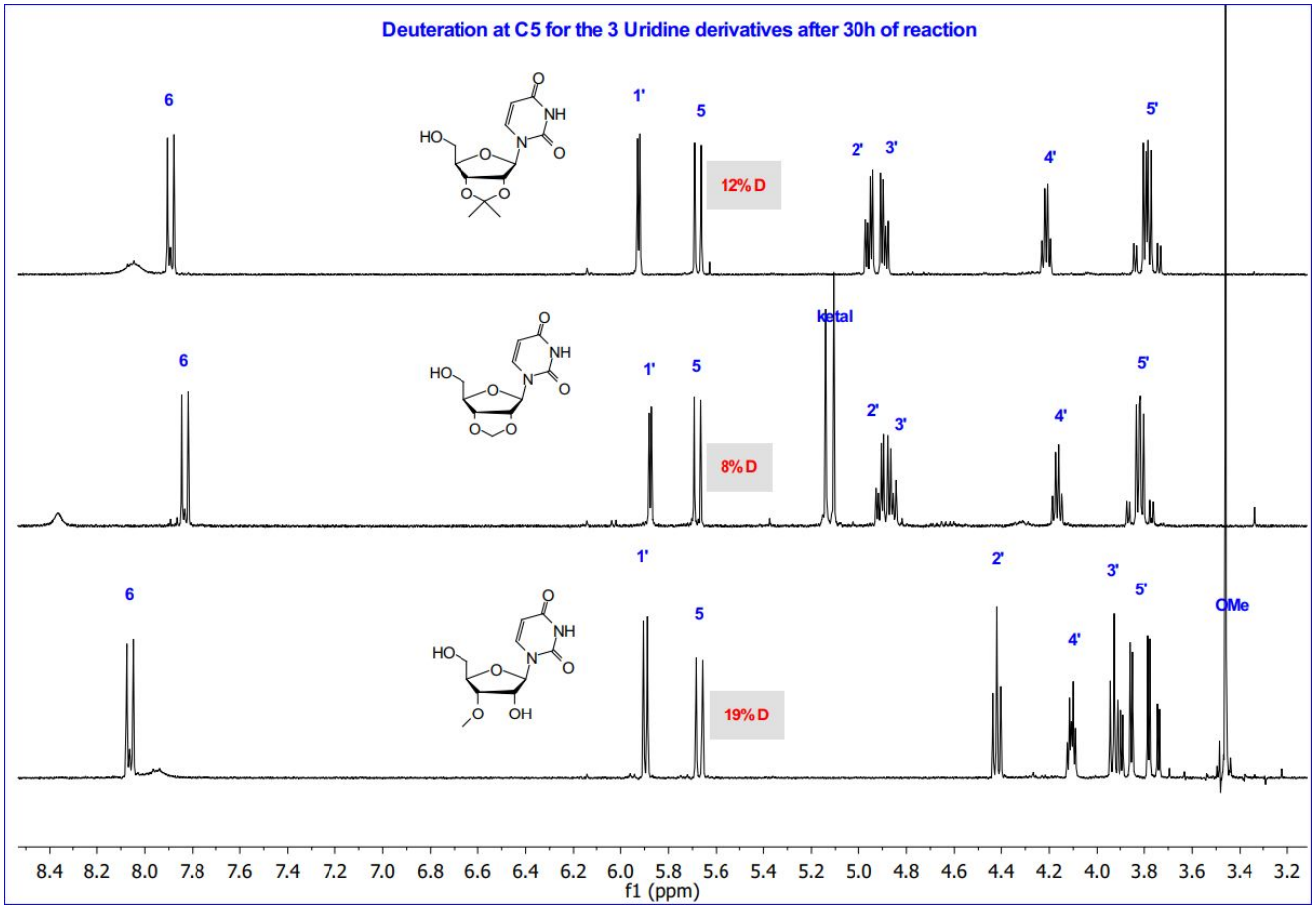

Figure S41 : Deuterium exchange experiments from dimethyl ketal **4**, methylene ketal **9** and 3'OMe Uridine.

Conditions: 16 µmoles of uridine derivatives were dissolved in 0.6mL of a stock solution of acetone/H_2SO_4 2mL/2 drops. Some Na_2SO_4 was added as a desiccant in the mixture.

Remark: the sulfuric acid content was purposely low to slow the kinetics of reaction and no stable O-cyclonucleoside is observed under these mildly acidic conditions that do not allow fast ketal exchange.

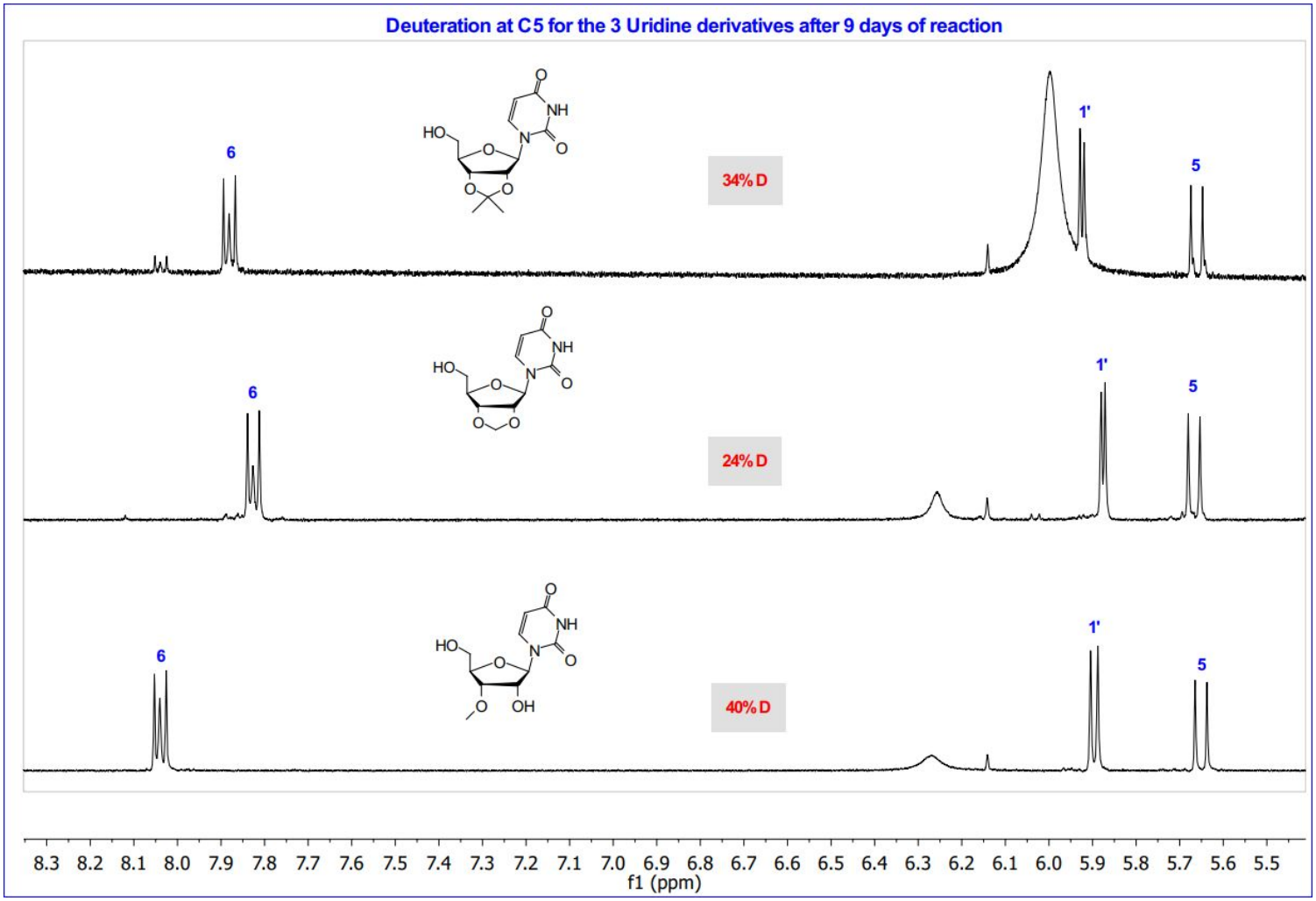

Figure S42 : Deuterium exchange experiments from dimethyl ketal **4**, methylene ketal **9** and 3'OMe Uridine after 30h of reaction.

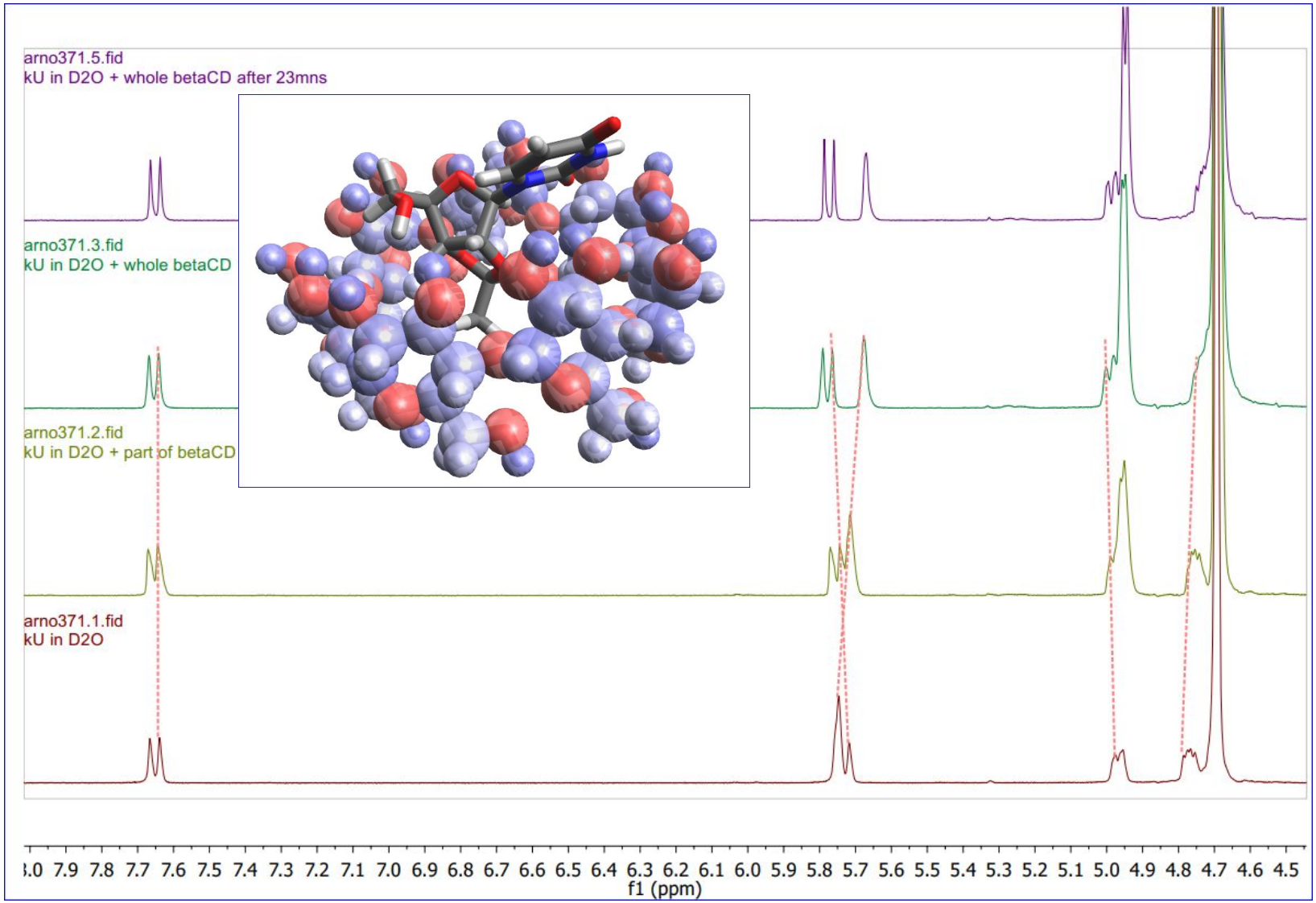

Figure S43 : Inclusion complex between dimethyl ketal uridine **4** and β-cyclodextrin.

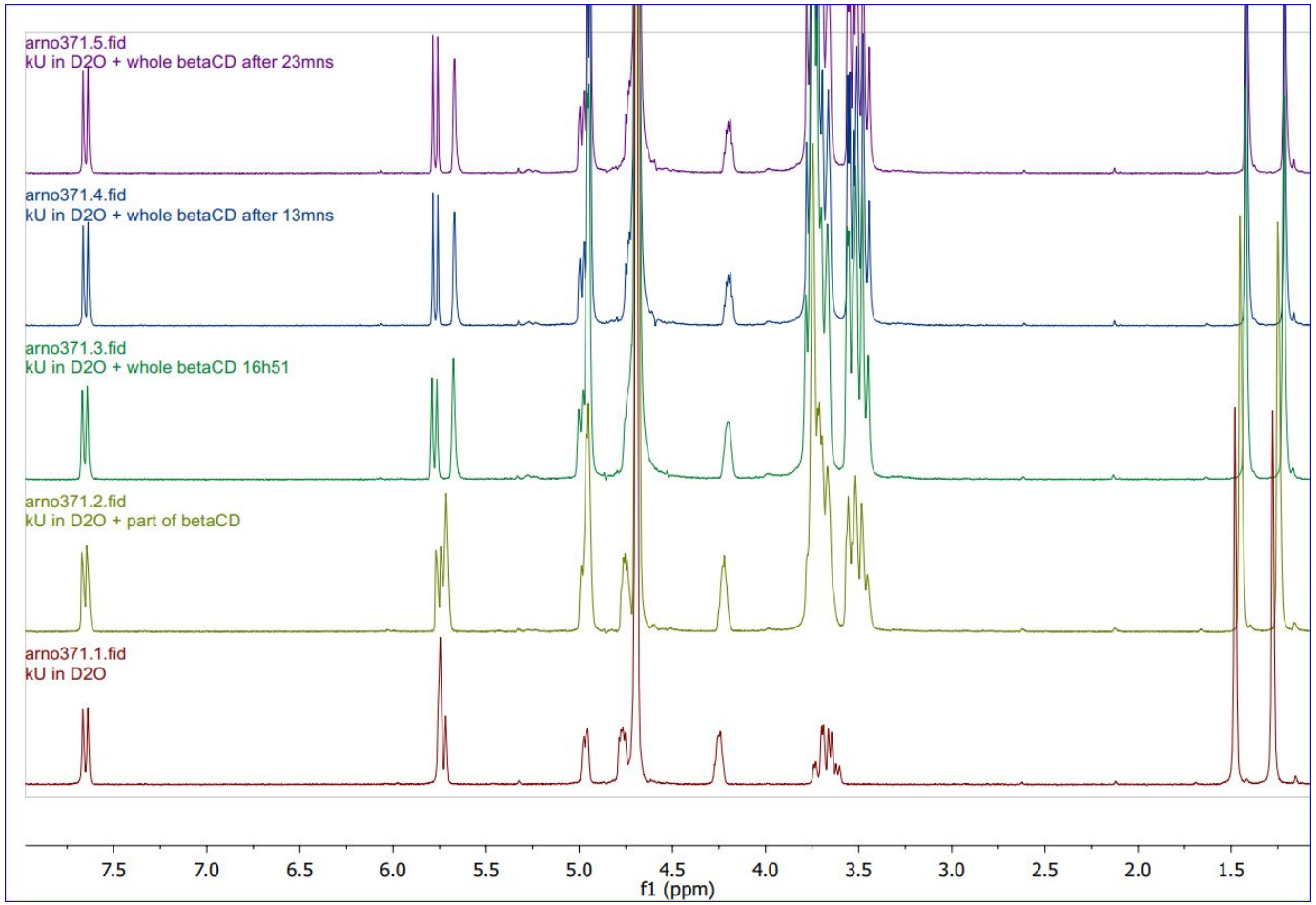

Figure S44 : Inclusion complex between dimethyl ketal uridine **4** and β-cyclodextrin.

The embedded ketal and H1' protons move upfield while the uracil H5 protons that are probably lying outside the cyclodextrin interior move downfield.